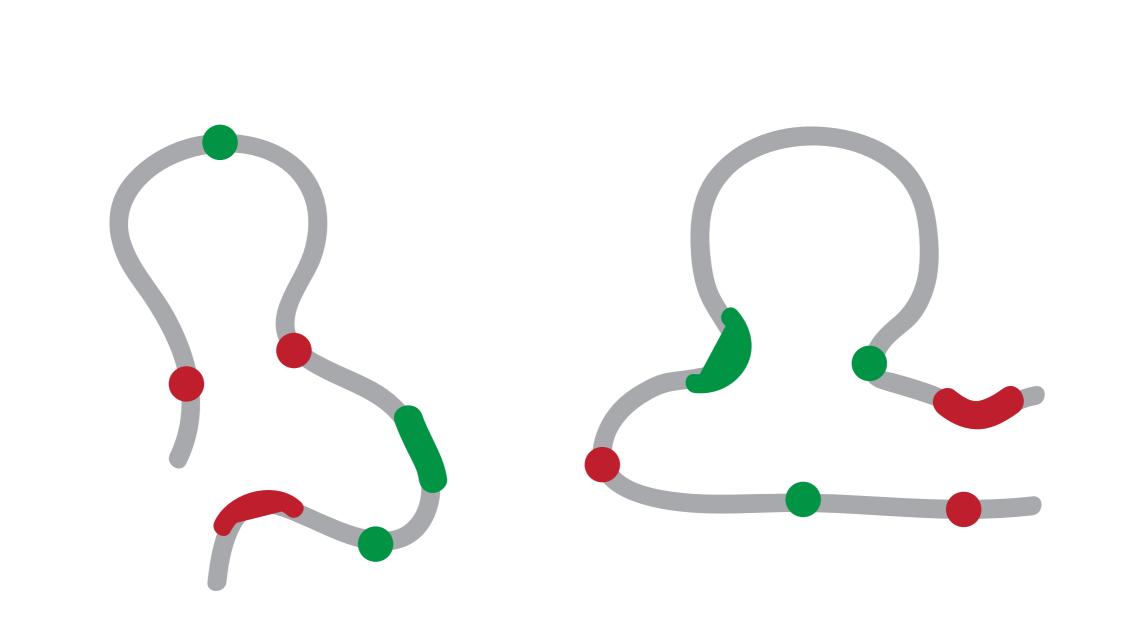
Structure determination of genomes and genomic domains by satisfaction of spatial restraints

Marc A. Marti-Renom
Structural Genomics Group (ICREA, CNAG-CRG)







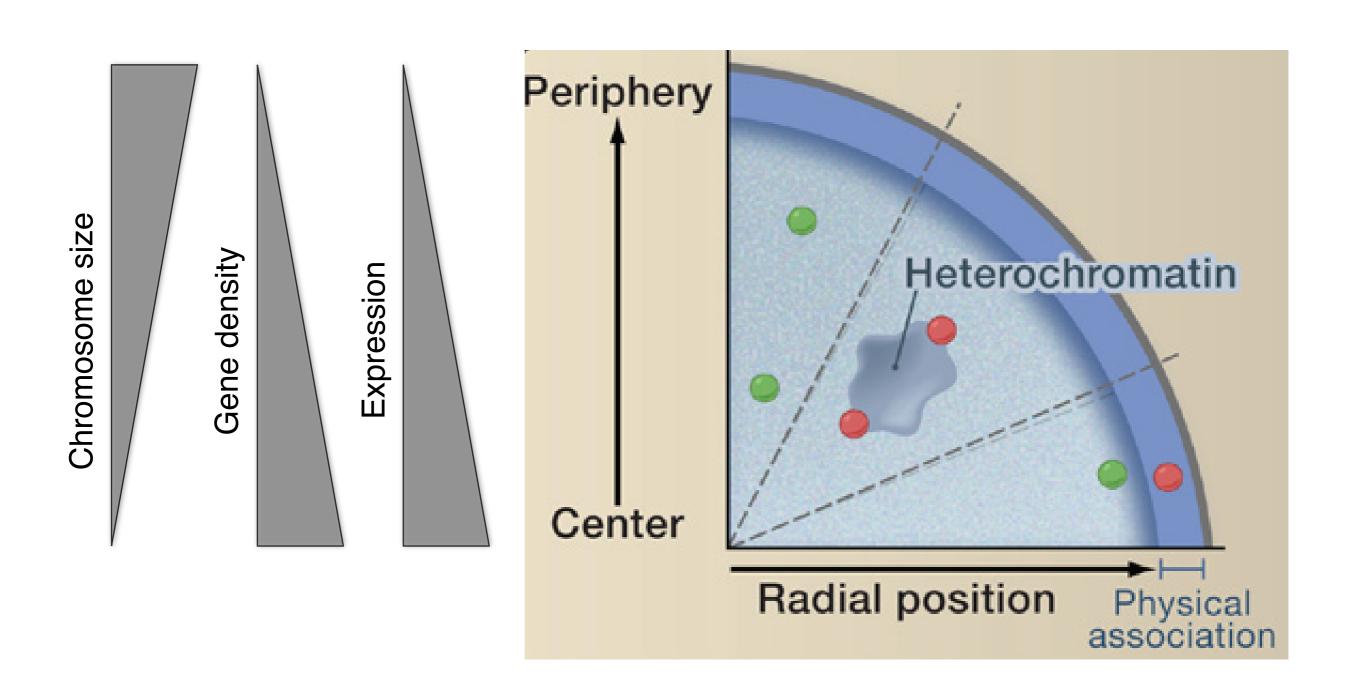
Resolution Gap

Marti-Renom, M. A. & Mirny, L. A. PLoS Comput Biol 7, e1002125 (2011)

Knowledge				
	IDA INA		1 20 3 14 18 7	12 15 6 10 Y 13 / 12 21 17 1 4 / 19 8 2 16 9 7 18
10° 10³	10 ⁶		DN/ 10	A length nt
				Volume
10 ⁻⁹ 10 ⁻⁶	10 ⁻³	10°		0^3 μm^3
				Time
10 ⁻¹⁰ 10 ⁻⁸ 10 ⁻⁶	10 ⁻⁴ 10 ⁻²	10°	10 ²	10 ³ s
			Re	solution
10 ⁻³	10 ⁻²		10 ⁻¹	μ

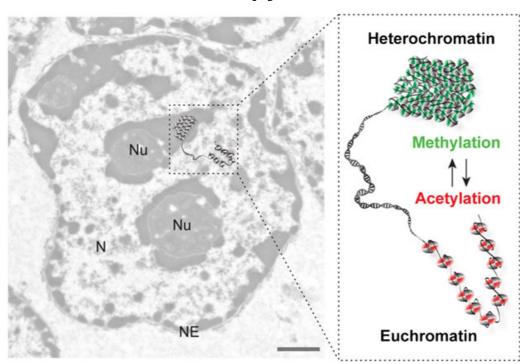
Level I: Radial genome organization

Takizawa, T., Meaburn, K. J. & Misteli, T. The meaning of gene positioning. Cell 135, 9–13 (2008).



Level II: Euchromatin vs heterochromatin

Electron microscopy



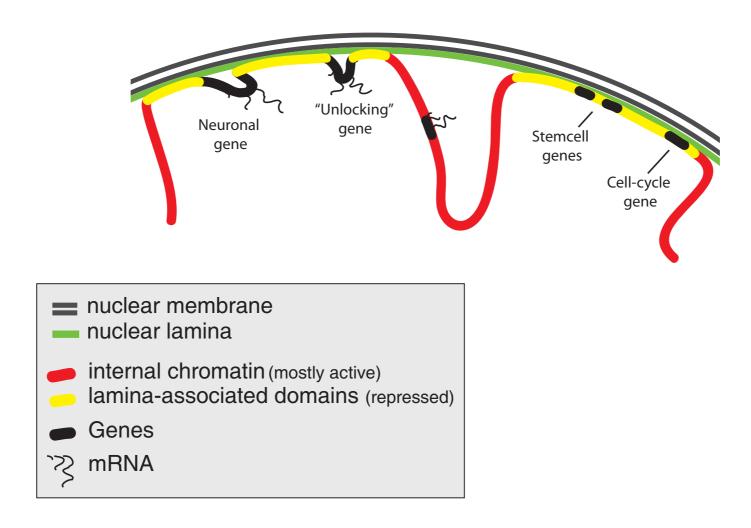
Euchromatin:

chromatin that is located away from the nuclear lamina, is generally less densely packed, and contains actively transcribed genes

Heterochromatin:

chromatin that is near the nuclear lamina, tightly condensed, and transcriptionally silent

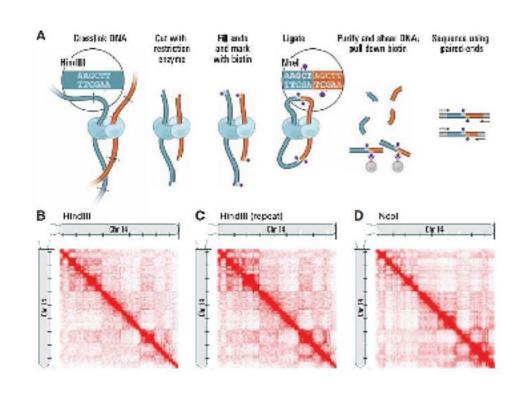
Level III: Lamina-genome interactions

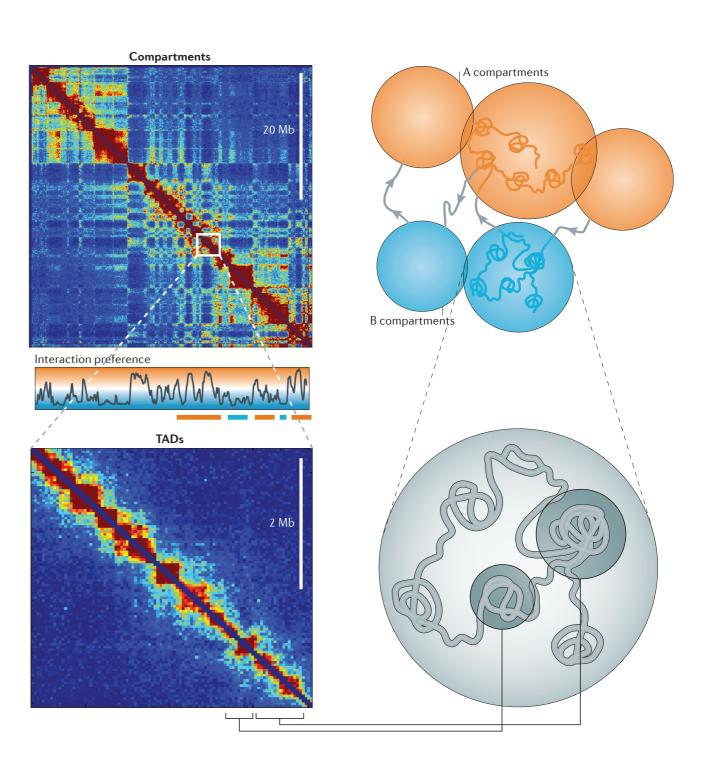


Most genes in Lamina Associated Domains are transcriptionally silent, suggesting that lamina-genome interactions are widely involved in the control of gene expression

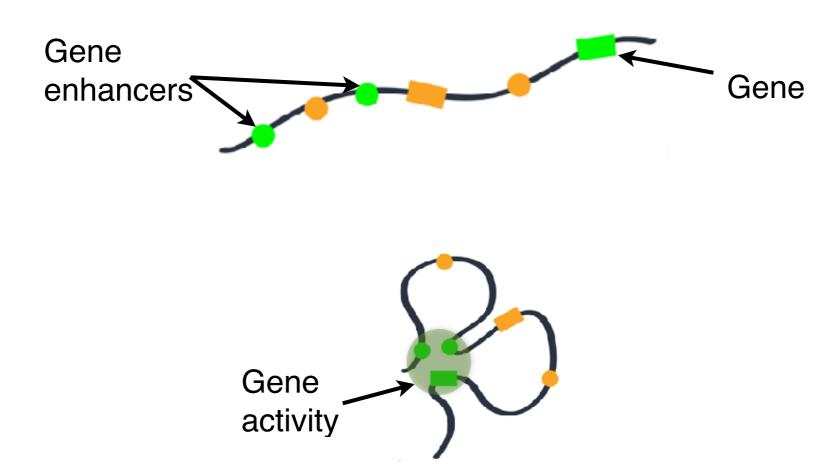
Level IV: Higher-order organization

Dekker, J., Marti-Renom, M. A. & Mirny, L. A. Nat Rev Genet 14, 390-403 (2013).





Level V: Chromatin loops



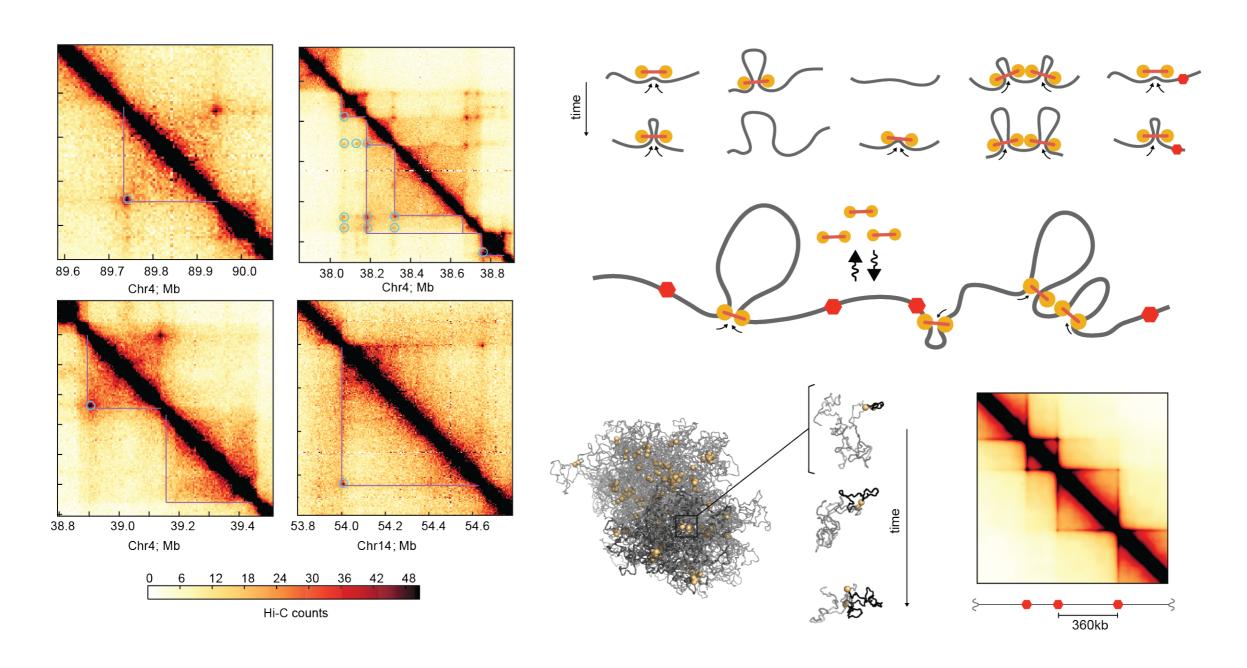
Loops bring distal genomic regions in close proximity to one another

This in turn can have profound effects on gene transcription

Enhancers can be thousands of kilobases away from their target genes in any direction (or even on a separate chromosome)

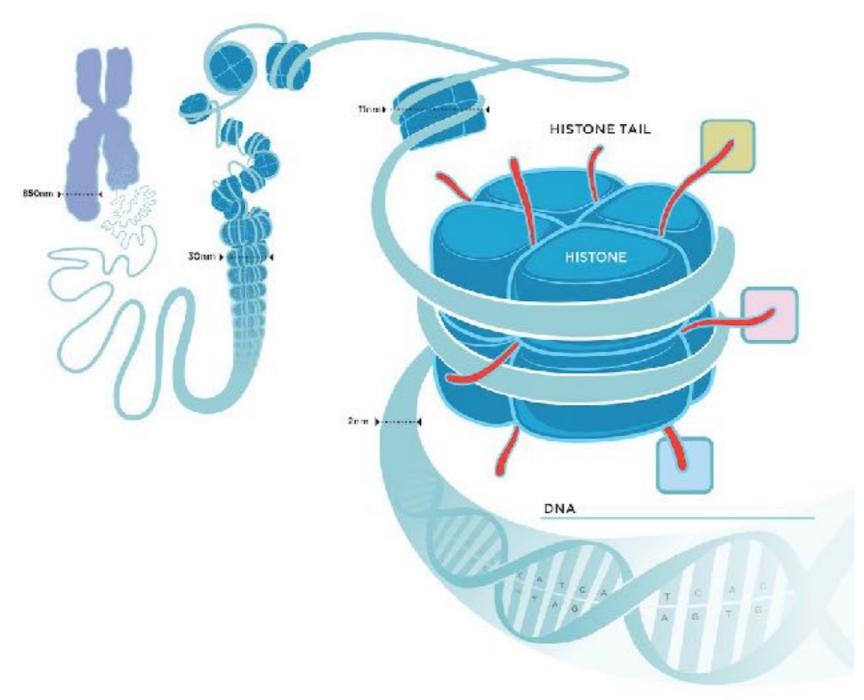
Level V: Loop-extrusion as a driving force

Fudenberg, G., Imakaev, M., Lu, C., Goloborodko, A., Abdennur, N., & Mirny, L. A. (2015). Formation of Chromosomal Domains by Loop Extrusion. bioRxiv.



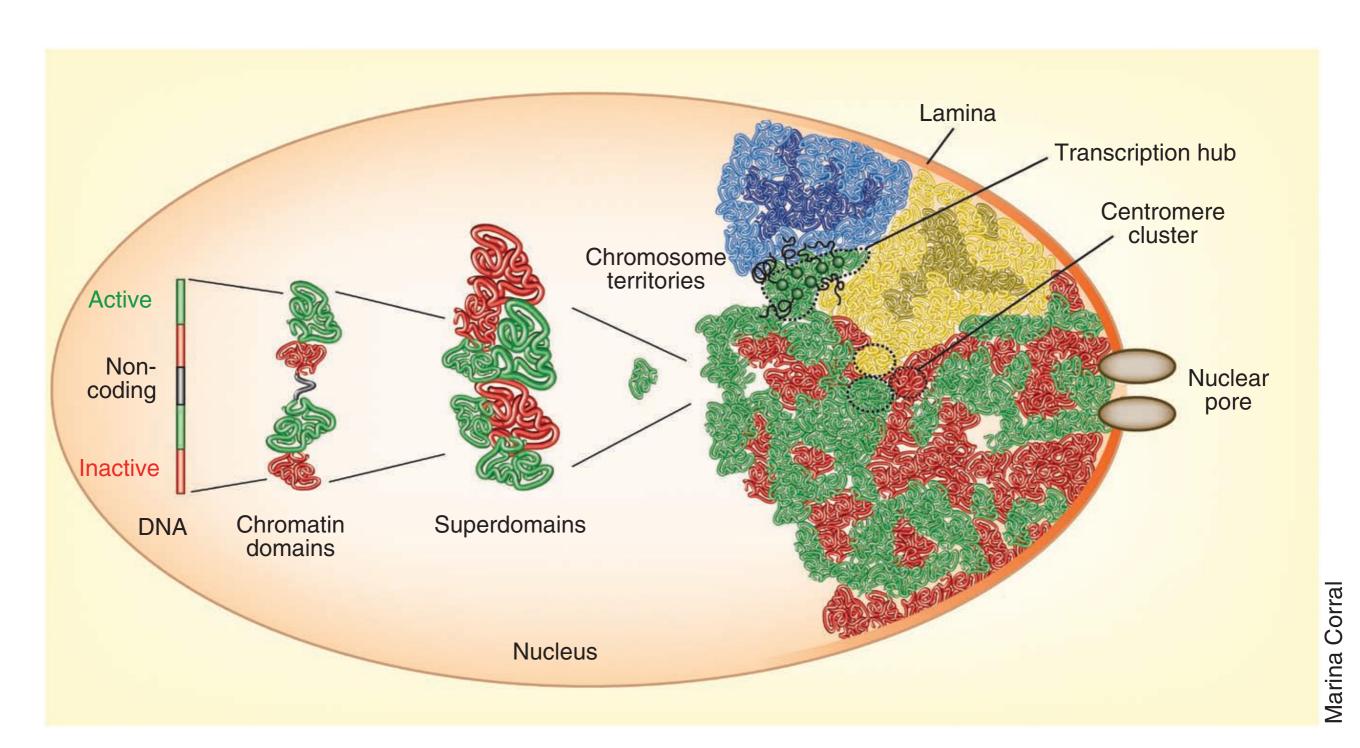
Level VI: Nucleosome

Chromosome Chromatin fibre Nucleosome

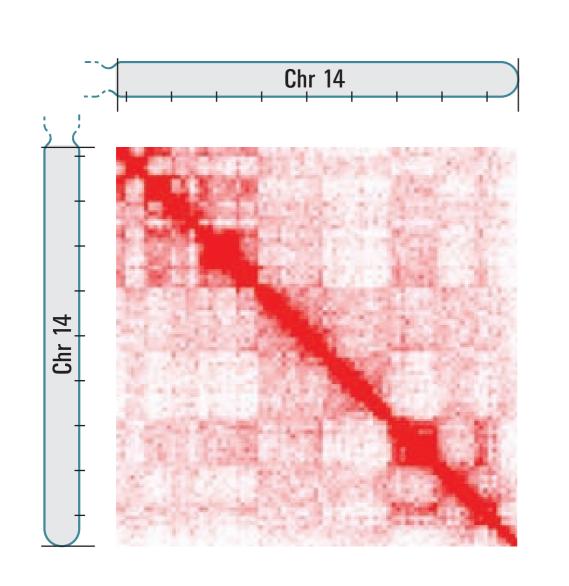


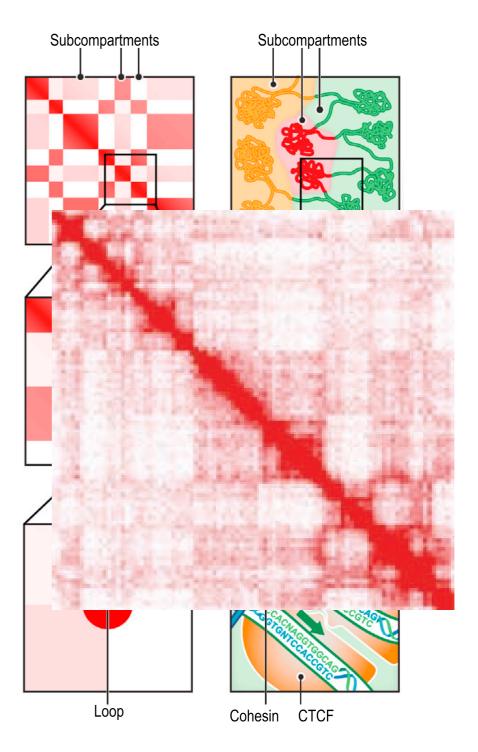
Complex genome organization

Cavalli, G. & Misteli, T. Functional implications of genome topology. Nat Struct Mol Biol 20, 290–299 (2013).



H chical genome organisation





Lieberman-Aiden, E., et al. (2009). Science, 326(5950), 289–293. Rao, S. S. P., et al. (2014). Cell, 1–29.

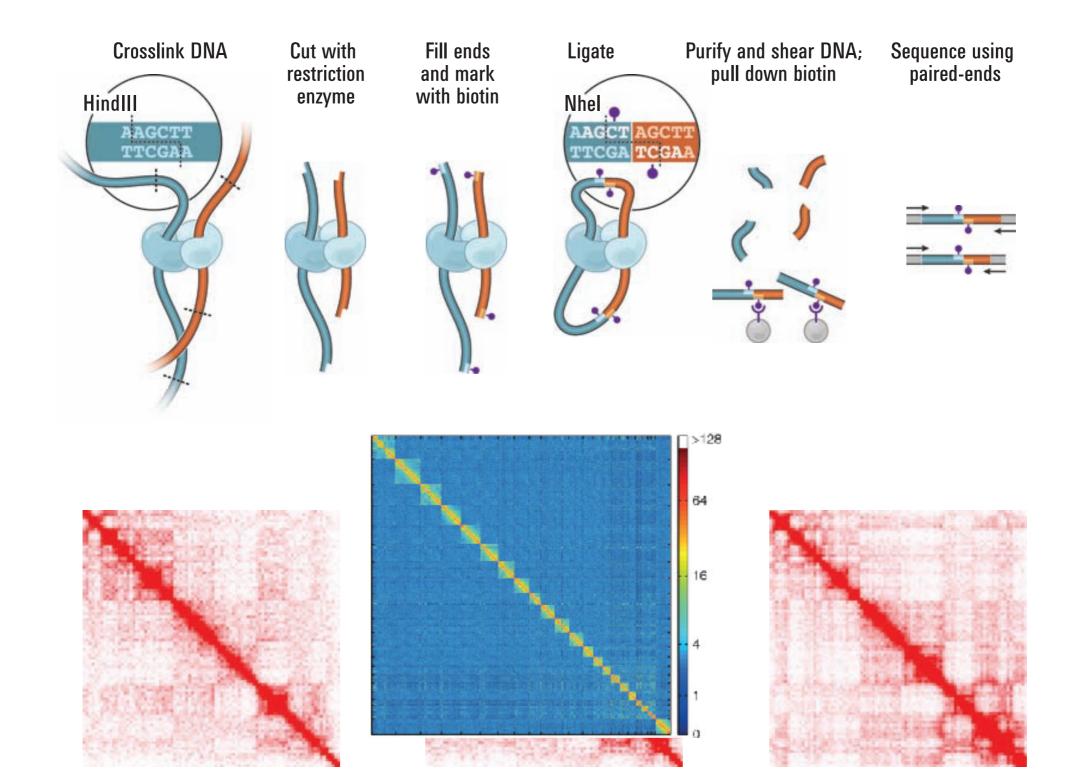
Resolution Gap

Marti-Renom, M. A. & Mirny, L. A. PLoS Comput Biol 7, e1002125 (2011)

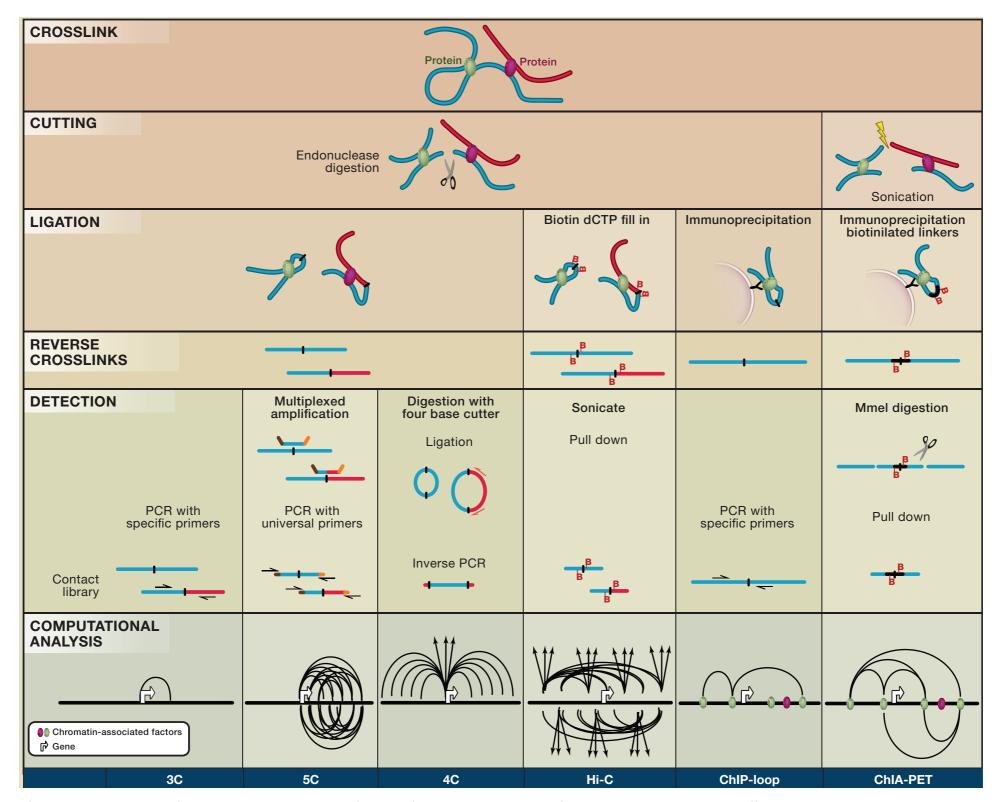
Knowledge				
	IDA INA		1 20 3 14 18 7	12 15 6 10 Y 13 / 12 21 17 1 4 / 19 8 2 16 9 7 18
10° 10³	10 ⁶		DN/ 10	A length nt
				Volume
10 ⁻⁹ 10 ⁻⁶	10 ⁻³	10°		0^3 μm^3
				Time
10 ⁻¹⁰ 10 ⁻⁸ 10 ⁻⁶	10 ⁻⁴ 10 ⁻²	10°	10 ²	10 ³ s
			Re	solution
10 ⁻³	10 ⁻²		10 ⁻¹	μ

Chromosome Conformation Capture

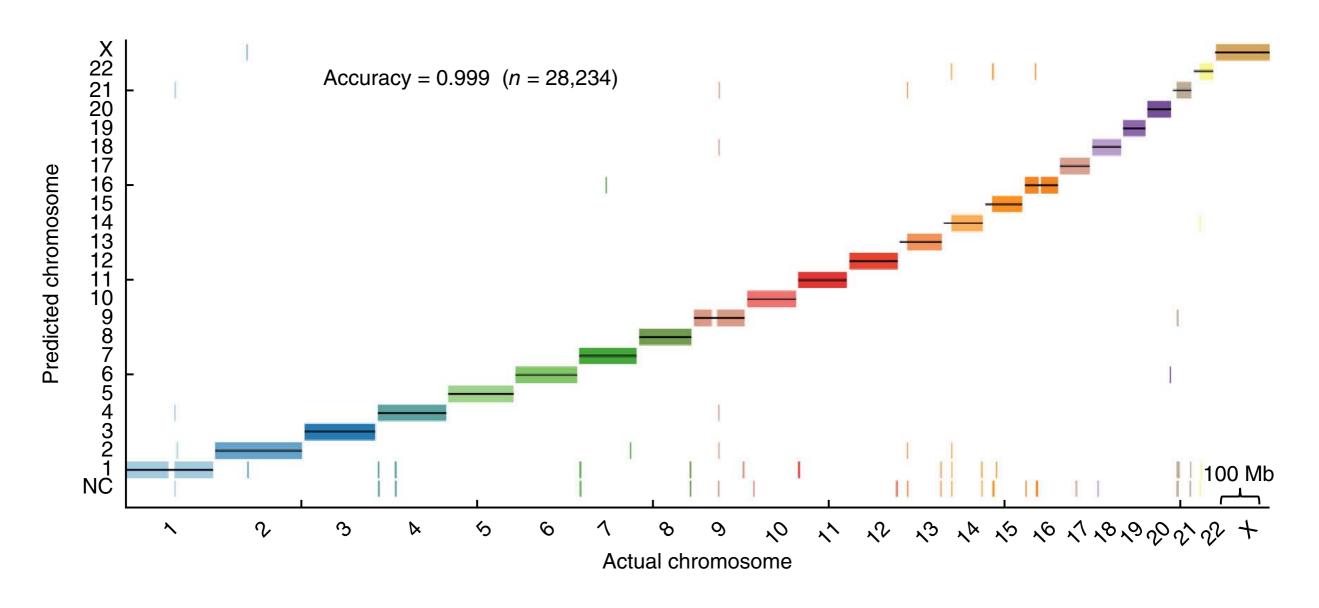
Dekker, J., Rippe, K., Dekker, M., & Kleckner, N. (2002). Science, 295(5558), 1306–1311. Lieberman-Aiden, E., et al. (2009). Science, 326(5950), 289–293.



Chromosome Conformation Capture



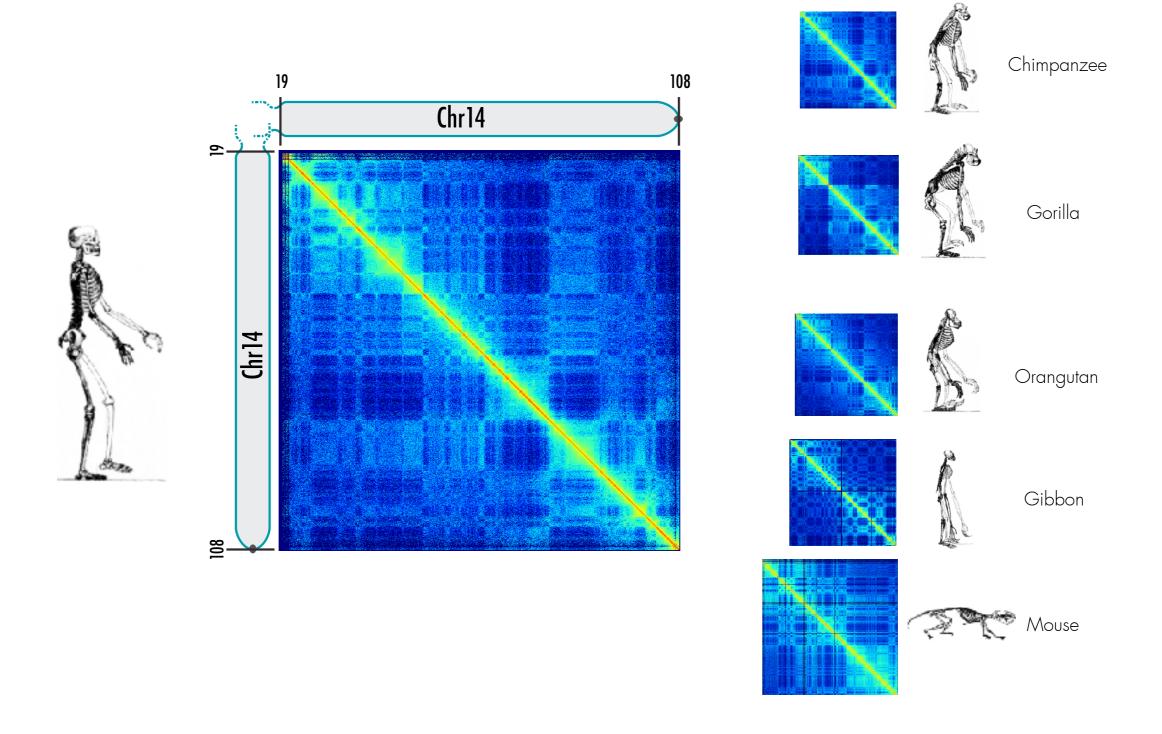
Hakim, O., & Misteli, T. (2012). SnapShot: Chromosome Confirmation Capture. Cell, 148(5), 1068–1068.e2.



Kaplan, N., & Dekker, J. (2013). High-throughput genome scaffolding from in vivo DNA interaction frequency. Nature

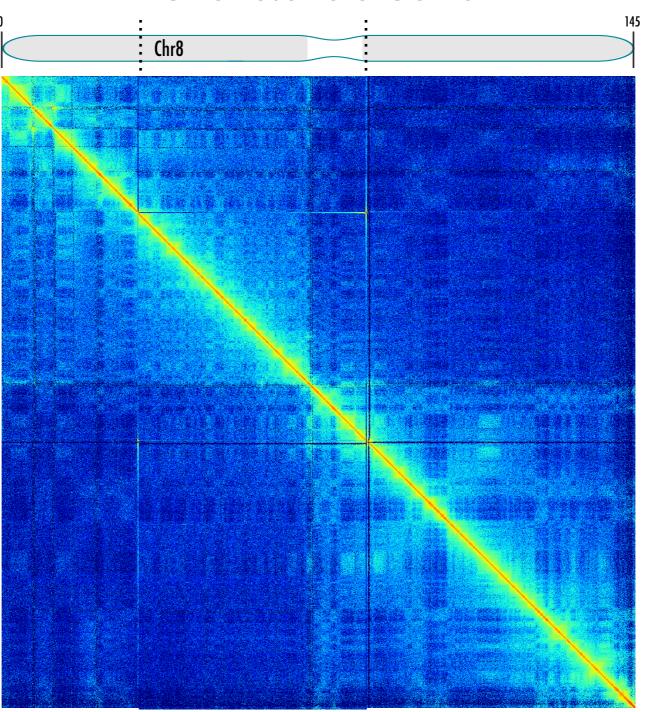
Great apes lymphoblast maps

Chromosome 14



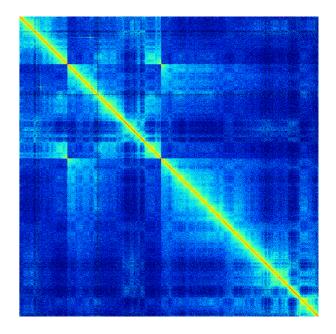
Assembly error detection

Chromosome 8 Gorilla



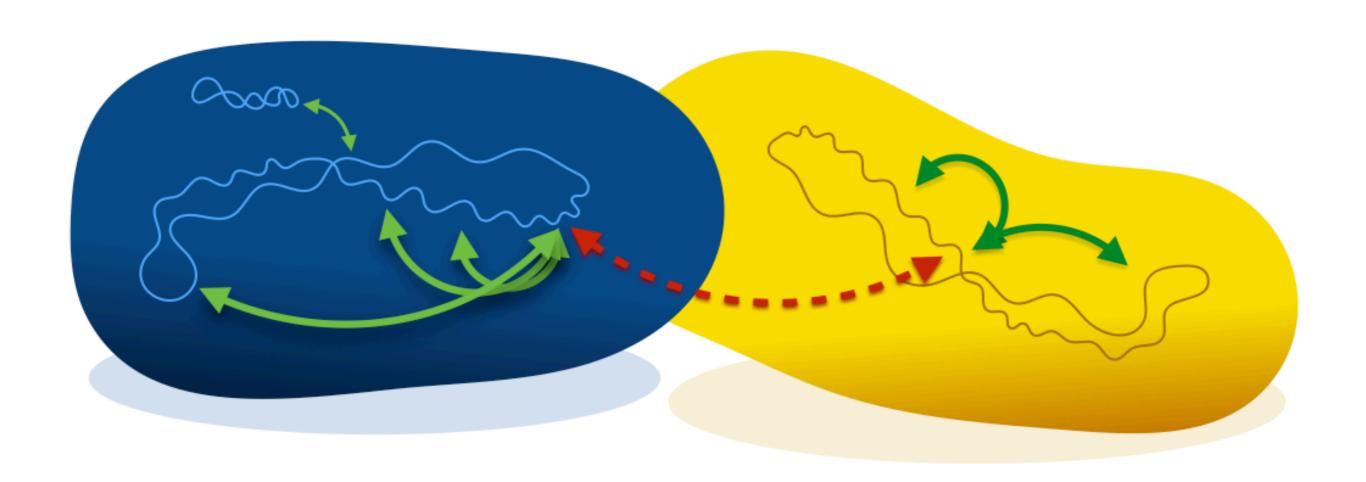
Chr 7

Chr 12



GGO8 has an inversion of the region corresponding to HSA8:30.0-86.9Mb Aylwyn Scally (Department of Genetics, University of Cambridge)

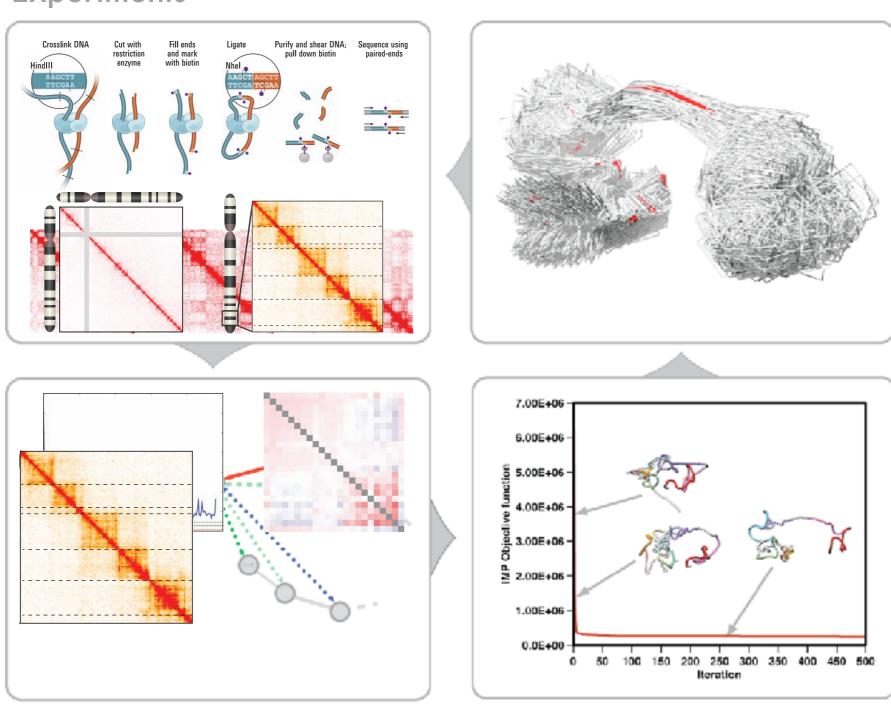
Chromosome Conformation Capture for meta genomics



Beitel, C. W., Froenicke, L., Lang, J. M., Korf, I. F., Michelmore, R. W., Eisen, J. A., & Darling, A. E. (2014). Strain- and plasmid-level deconvolution of a synthetic metagenome by sequencing proximity ligation products. doi:10.7287/peerj.preprints.260v1

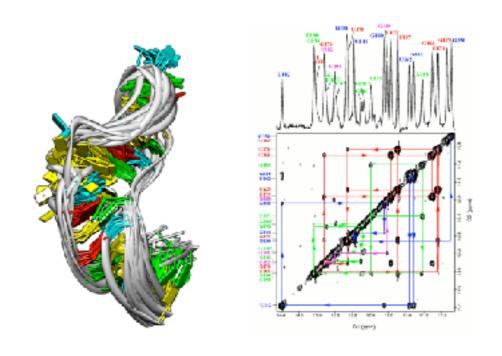
Hybrid Method Baù, D. & Marti-Renom, M. A. Methods 58, 300–306 (2012).

Experiments

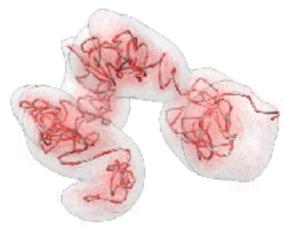


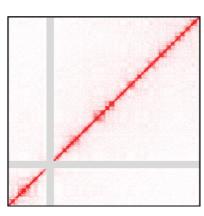
Computation

Structure determination using Hi-C data



Biomolecular structure determination 2D-NOESY data

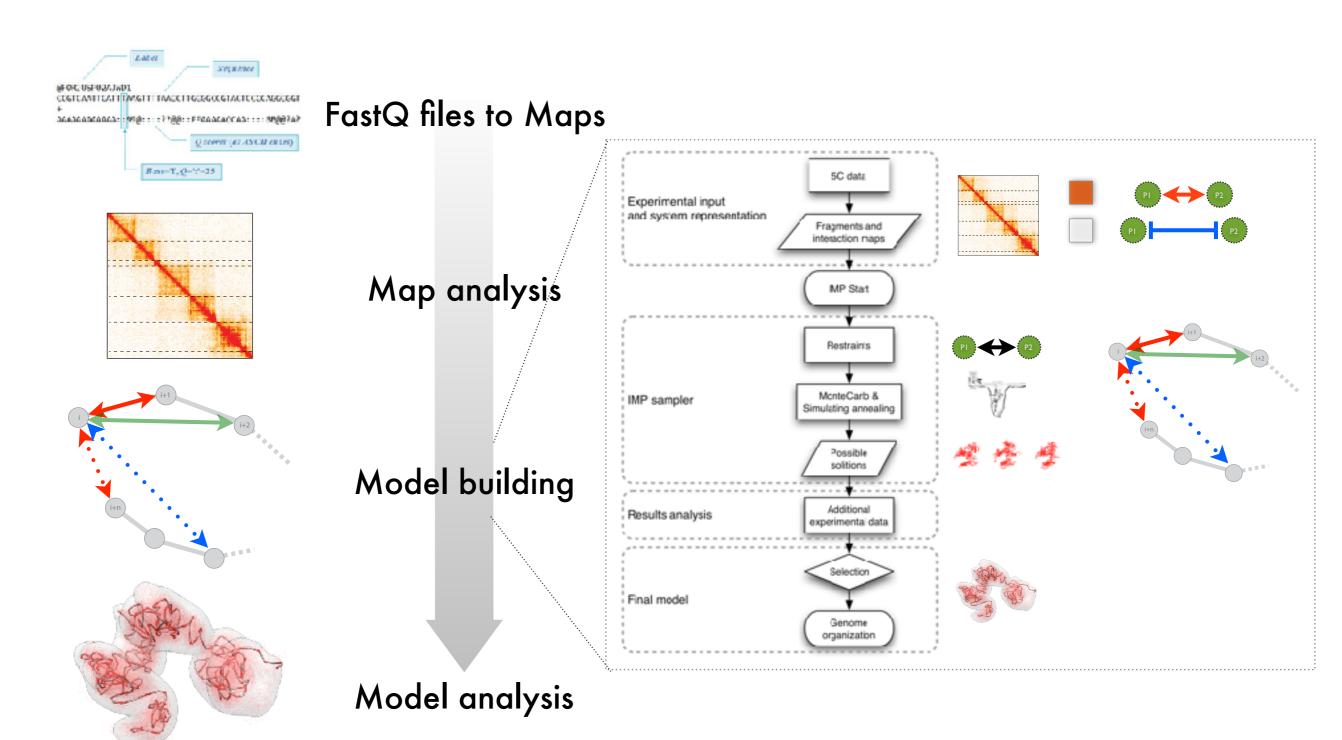




Chromosome structure determination 3C-based data



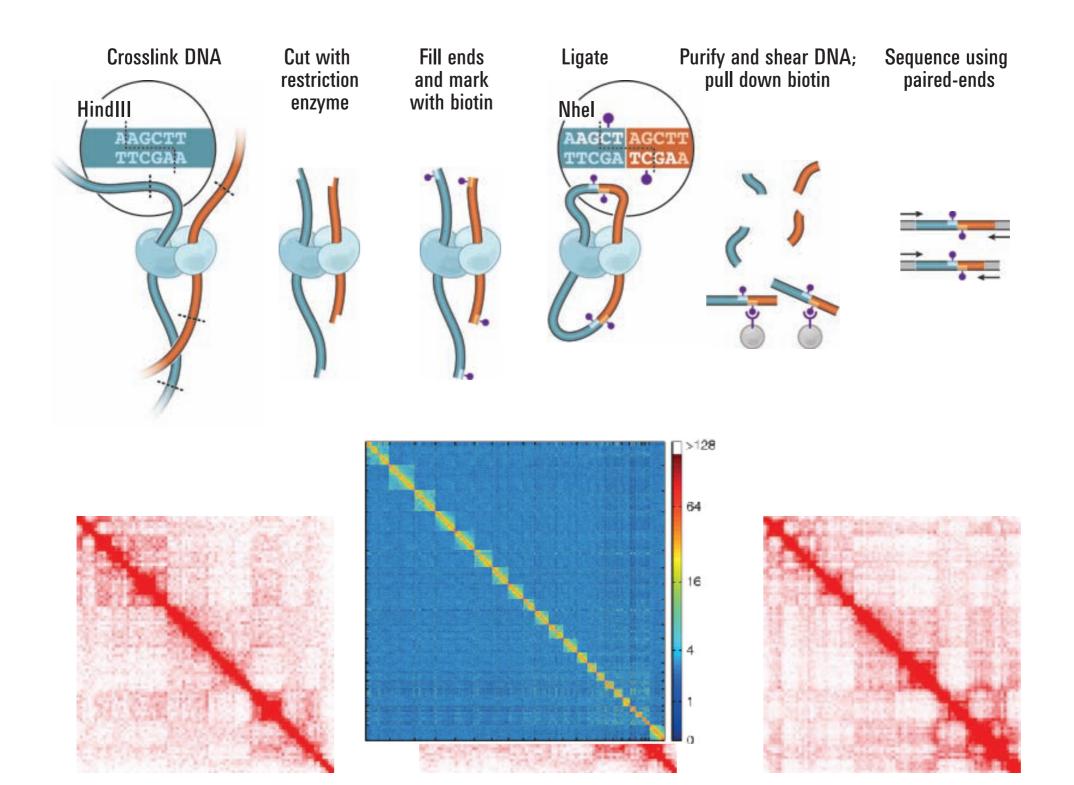
http://3DGenomes.org





Hi-C experiment

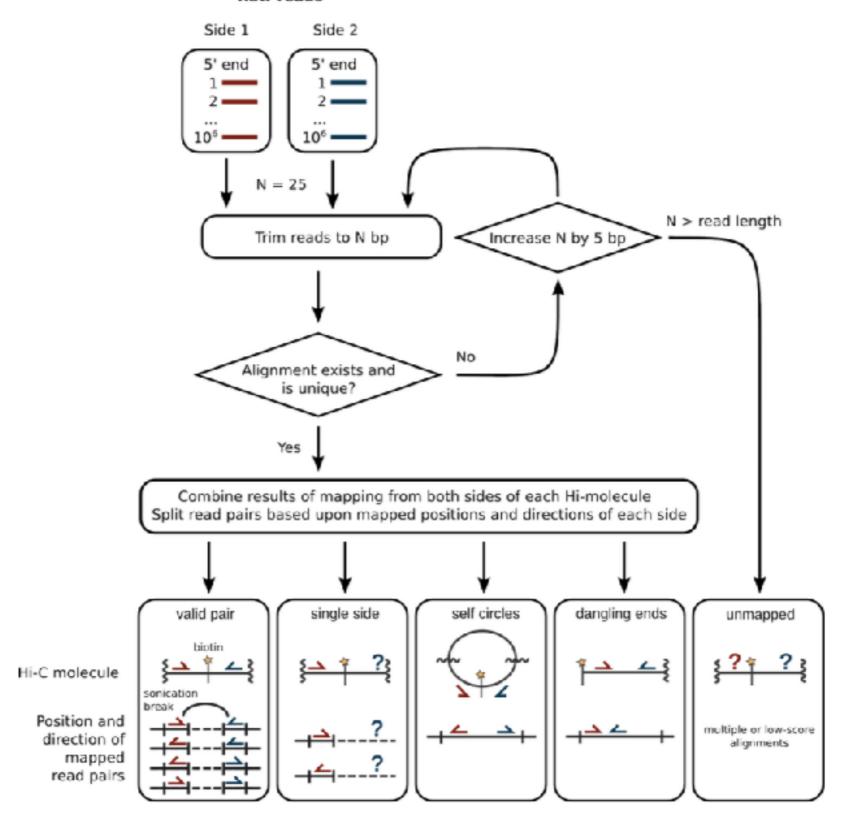
Lieberman-Aiden, E., et al. (2009). Science, 326(5950), 289–293.

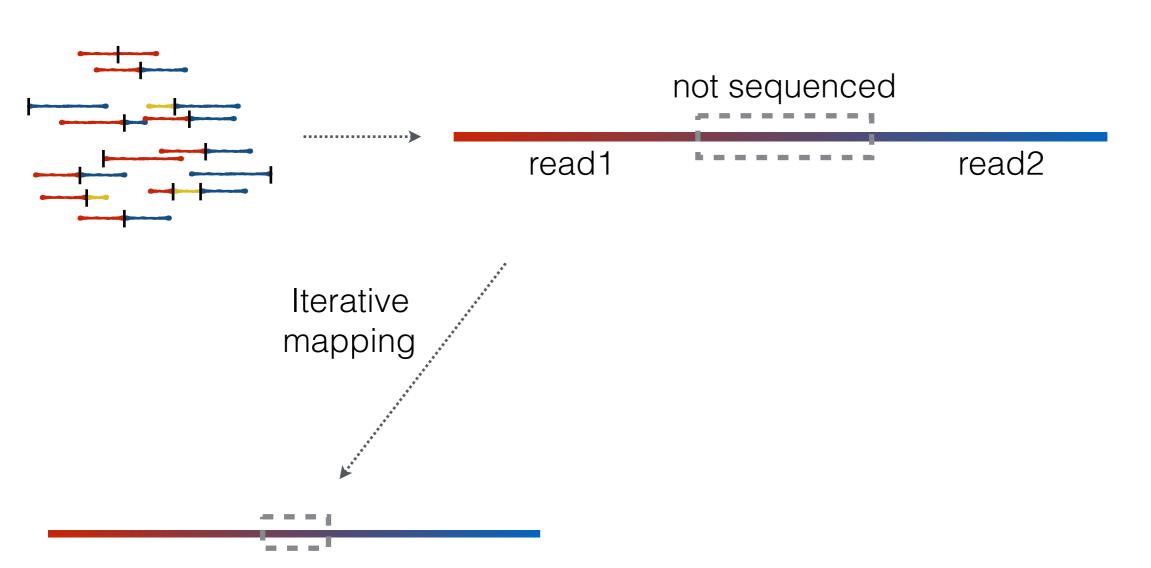


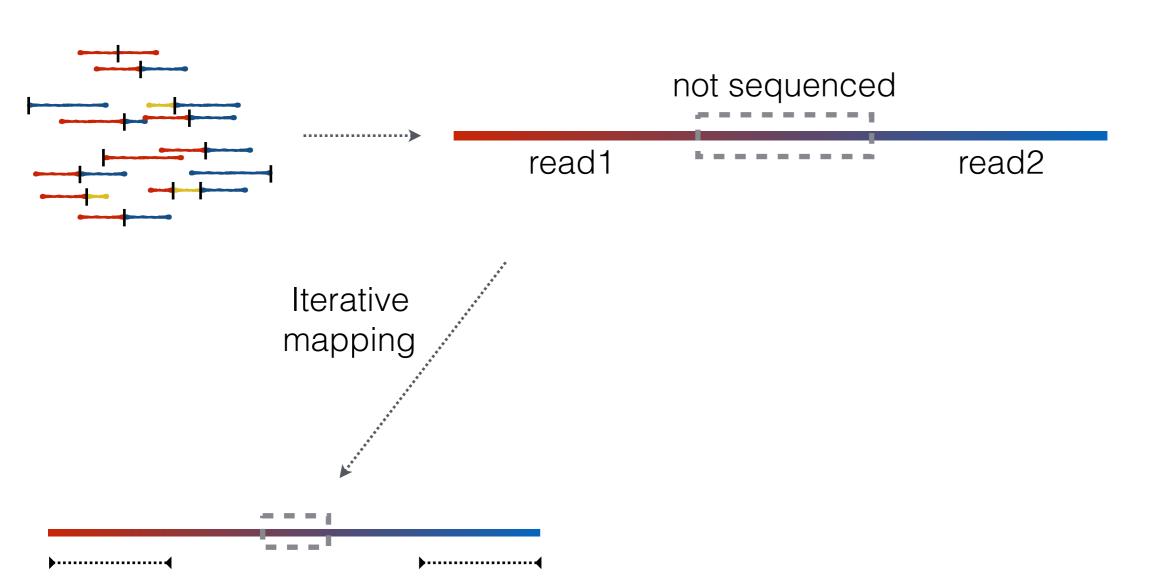
Mapping & Filtering

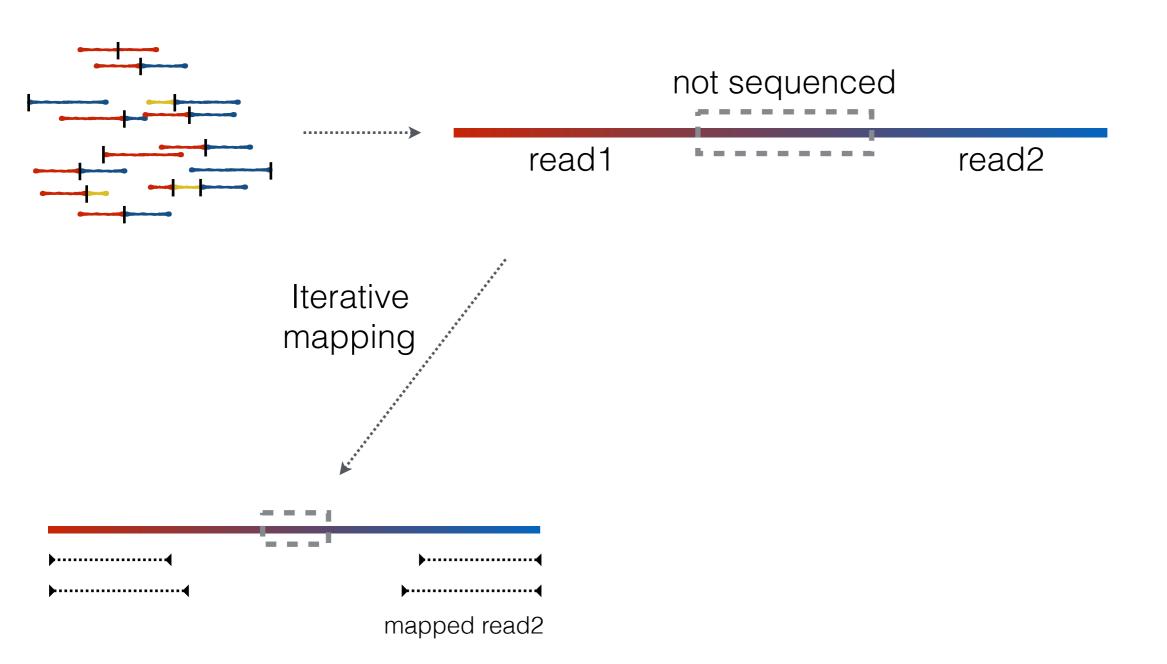
Imakaev, M. V et al. (2012). Nature Methods, 9(10), 999-1003.

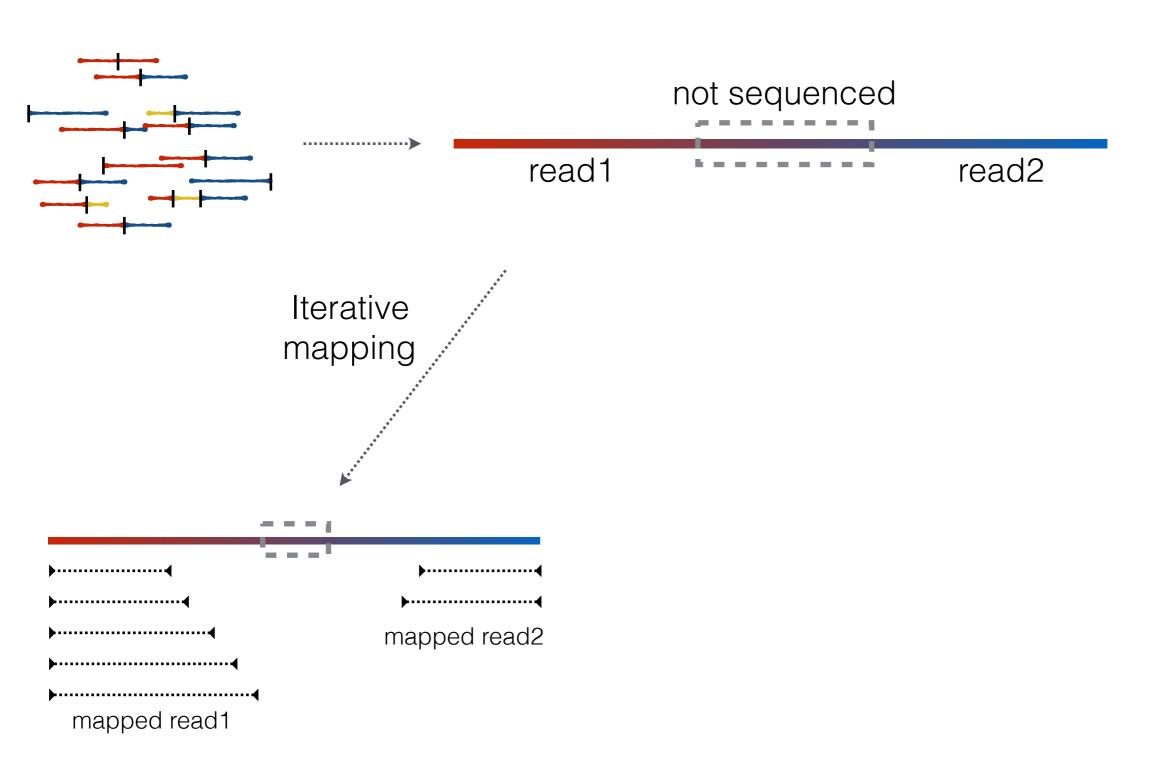
Raw reads

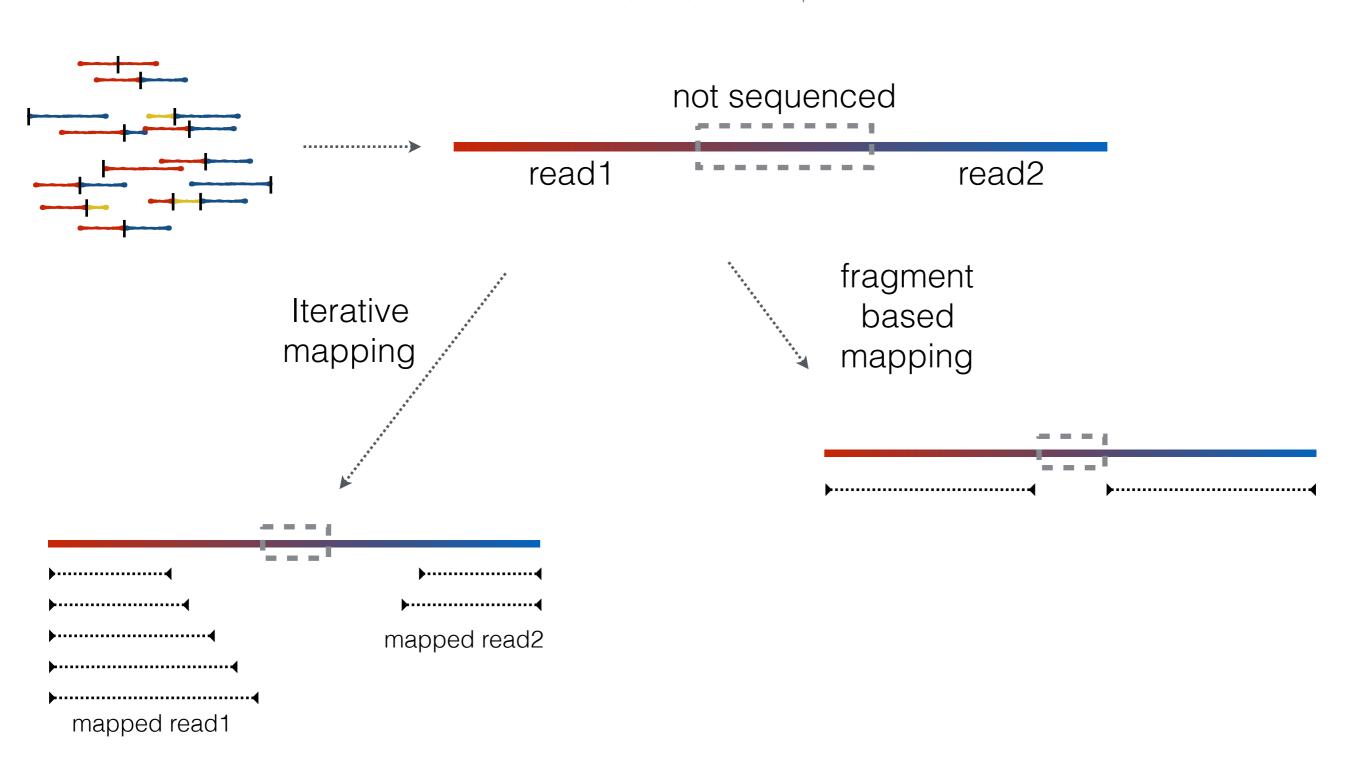


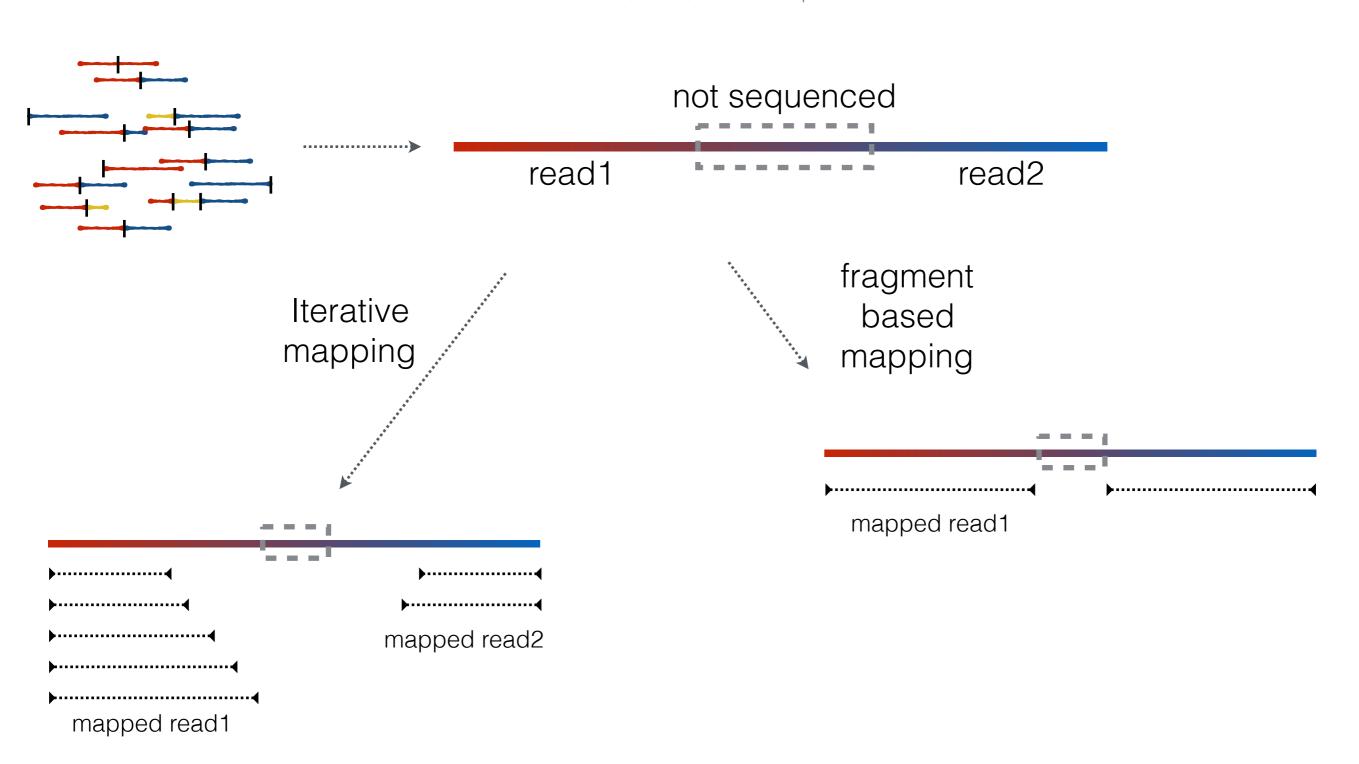


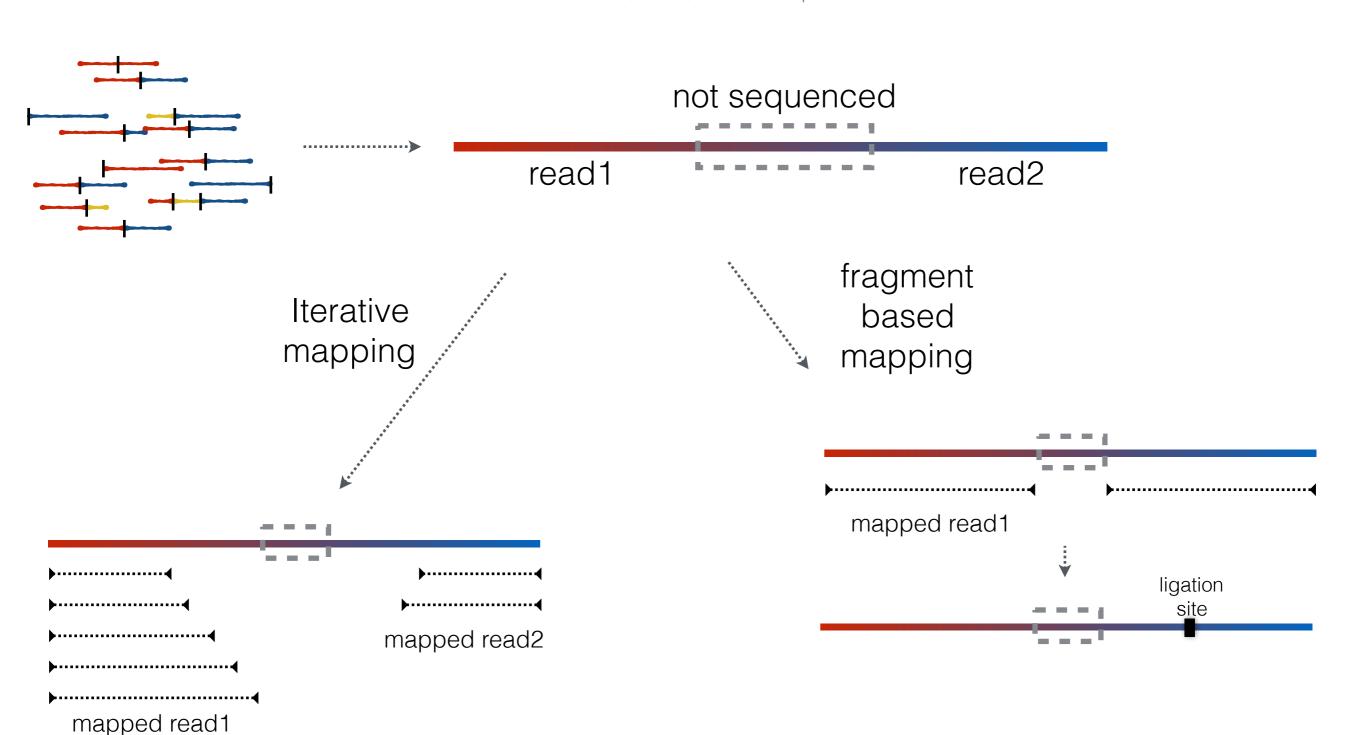


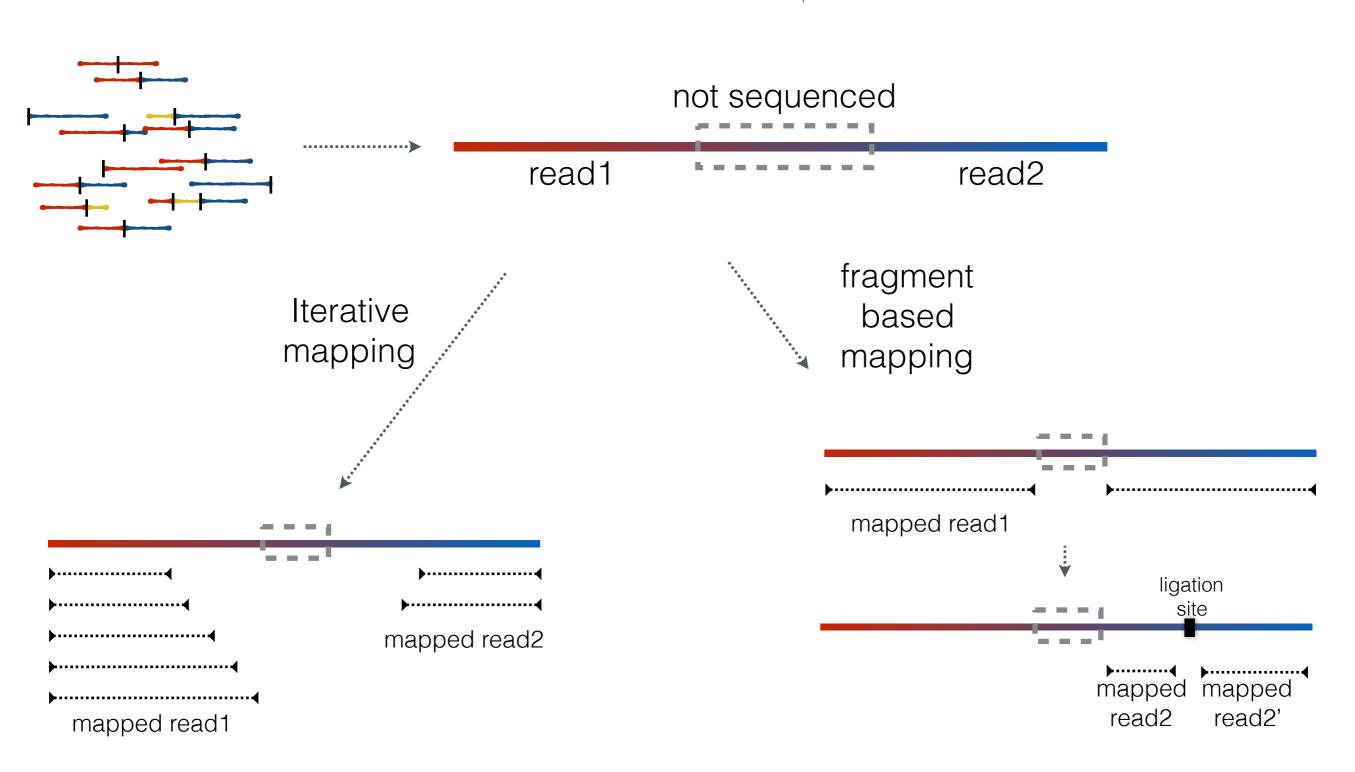


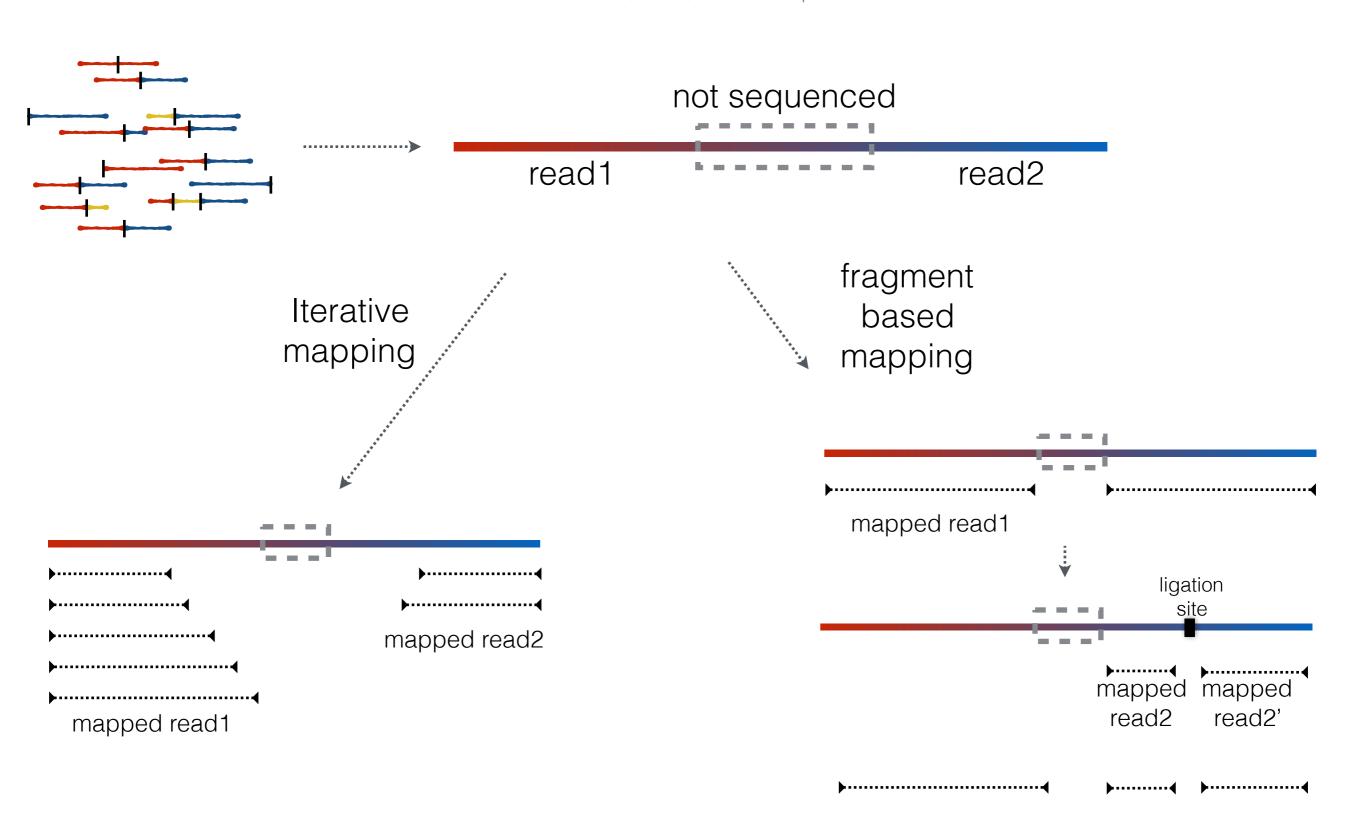








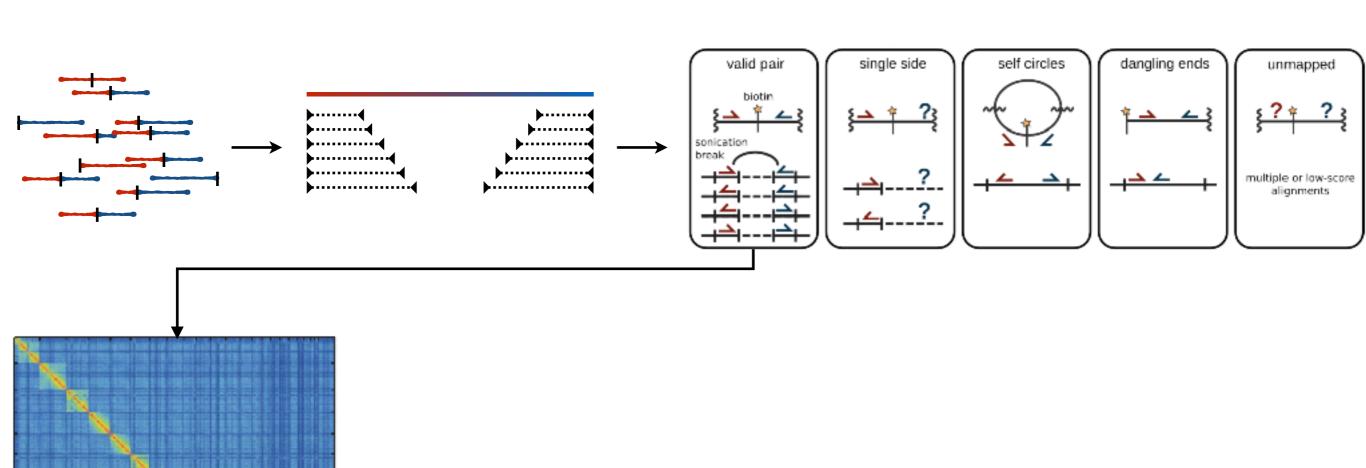


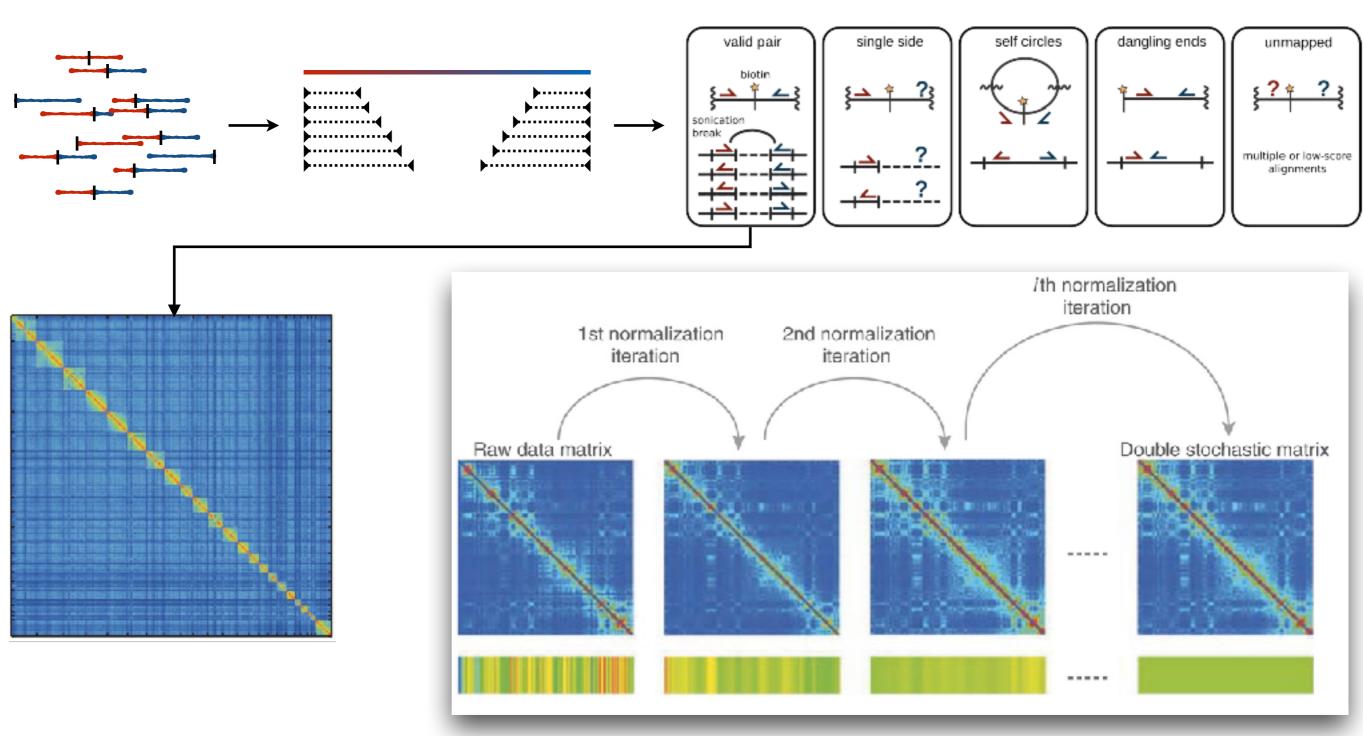


How much you normally map?

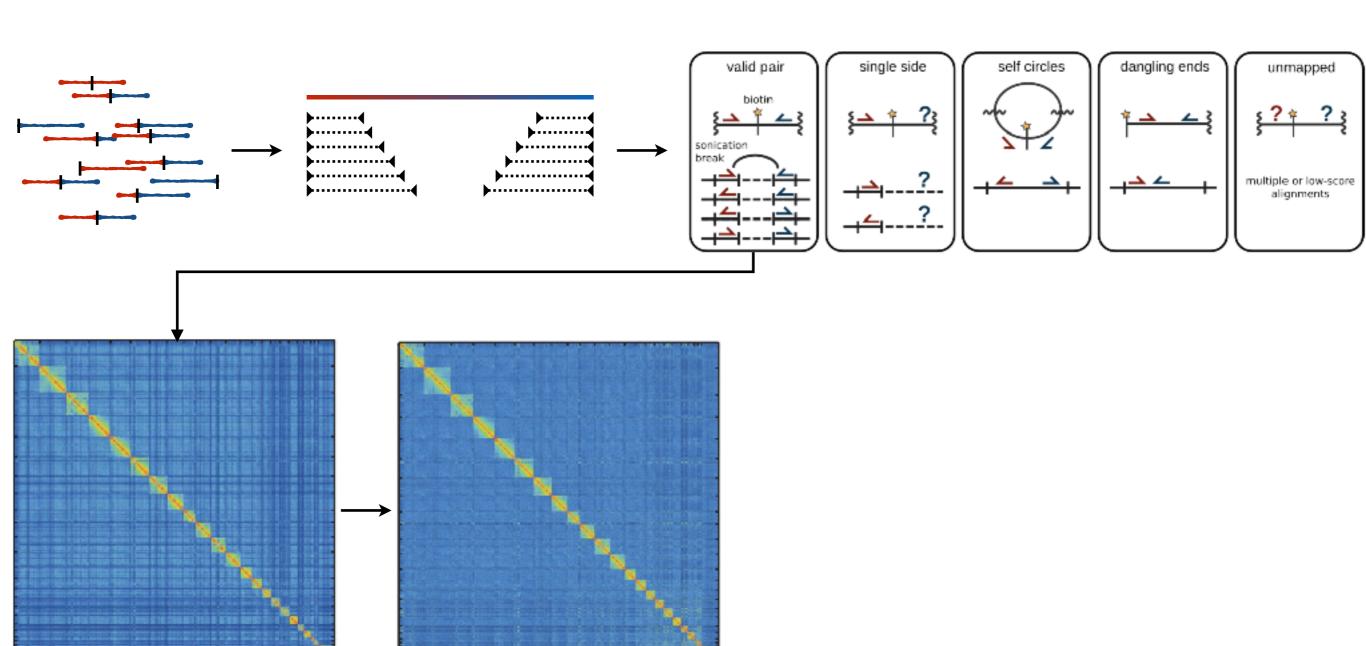
- 80-90% each end => 60-80% intersection
- ~1% multiple contacts
- Many of intersecting pairs will be lost in filtering...
- Final 40-60% of valid pairs
- One measure of quality is the CIS/TRANS ration (70-80% good)

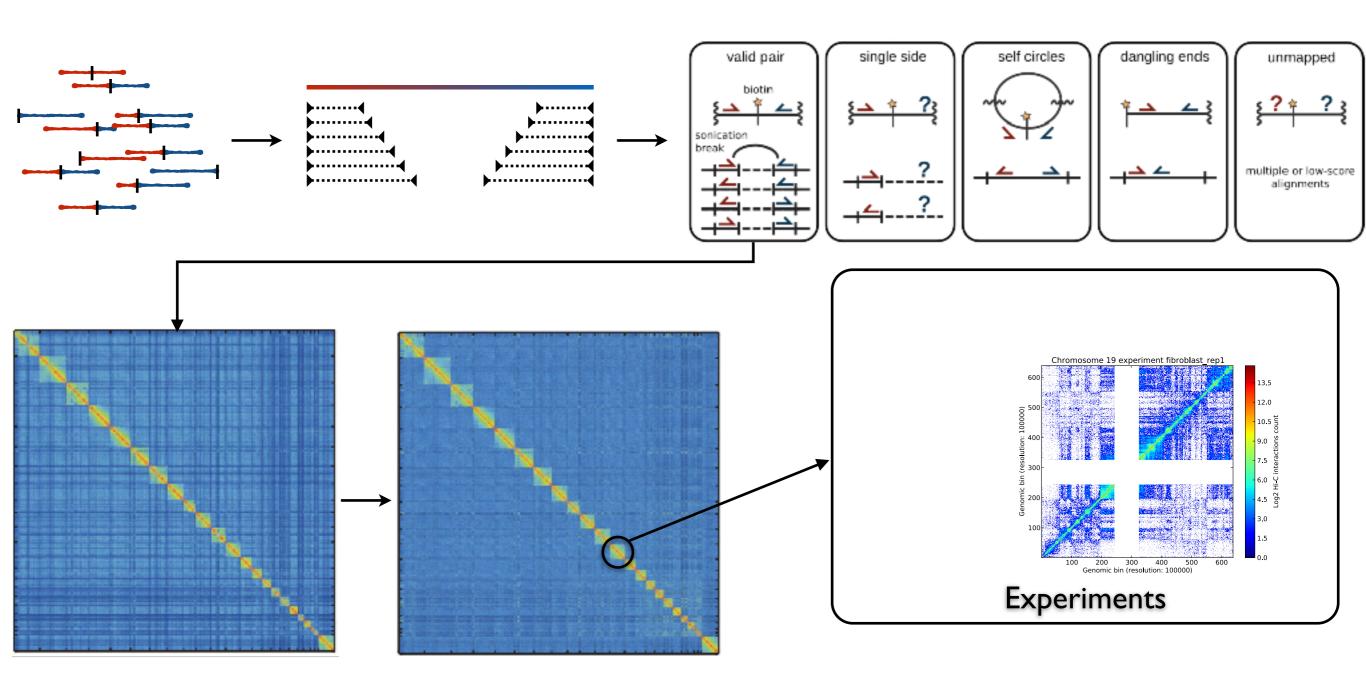


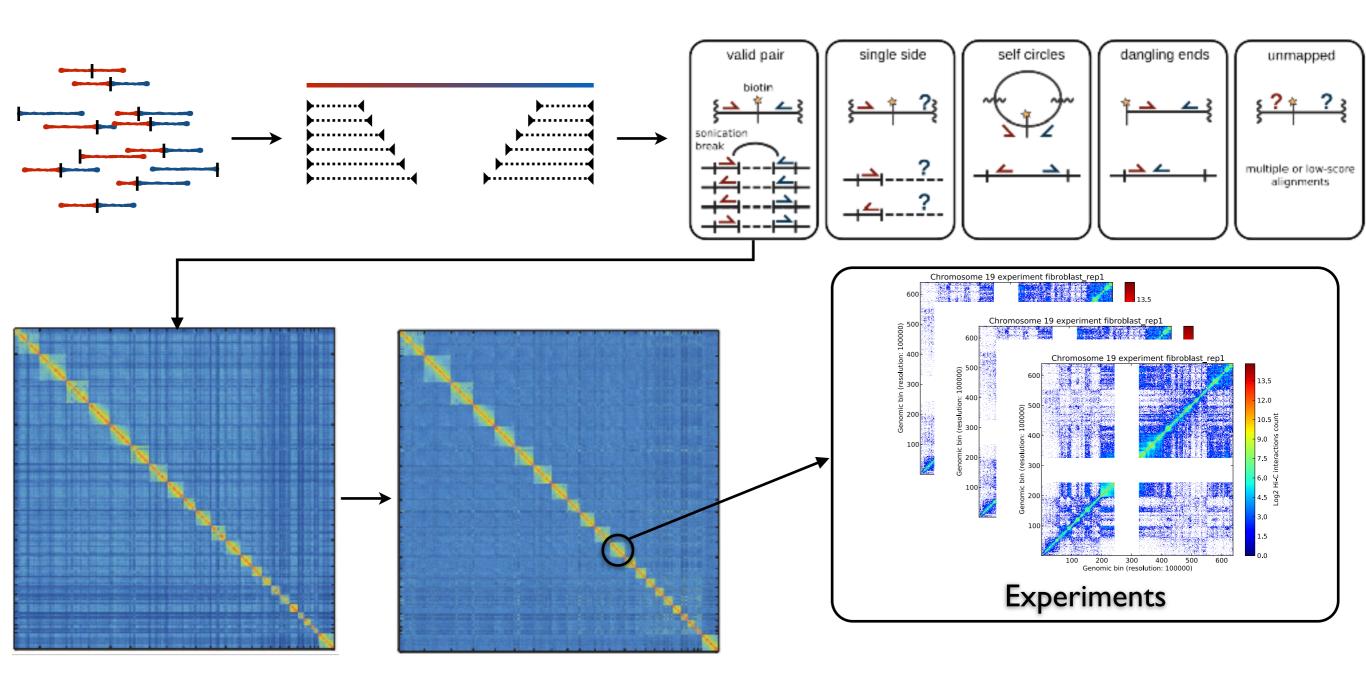


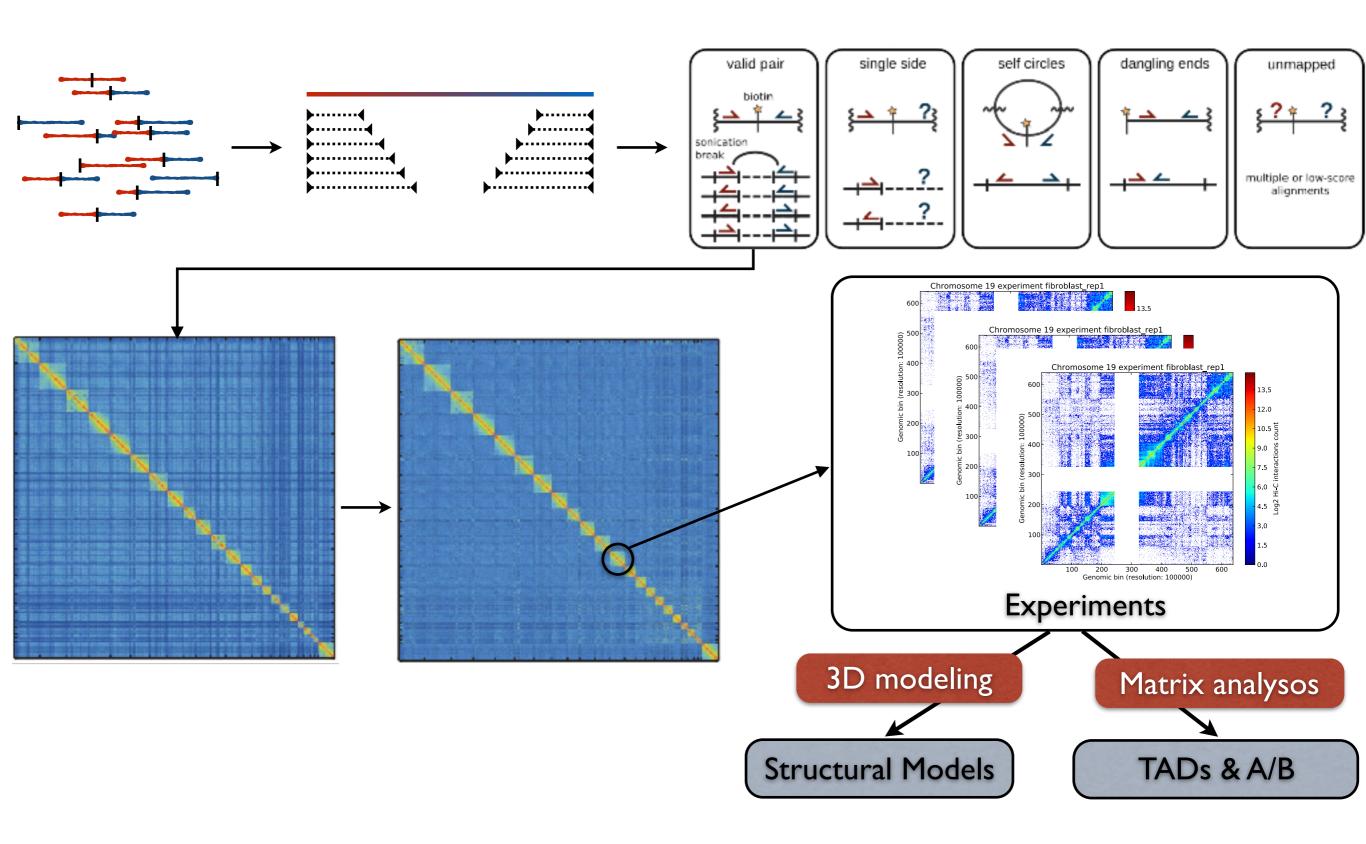


Zooming in on genome organization. Zhou, X. J., & Alber, F. Nature Methods (2012)

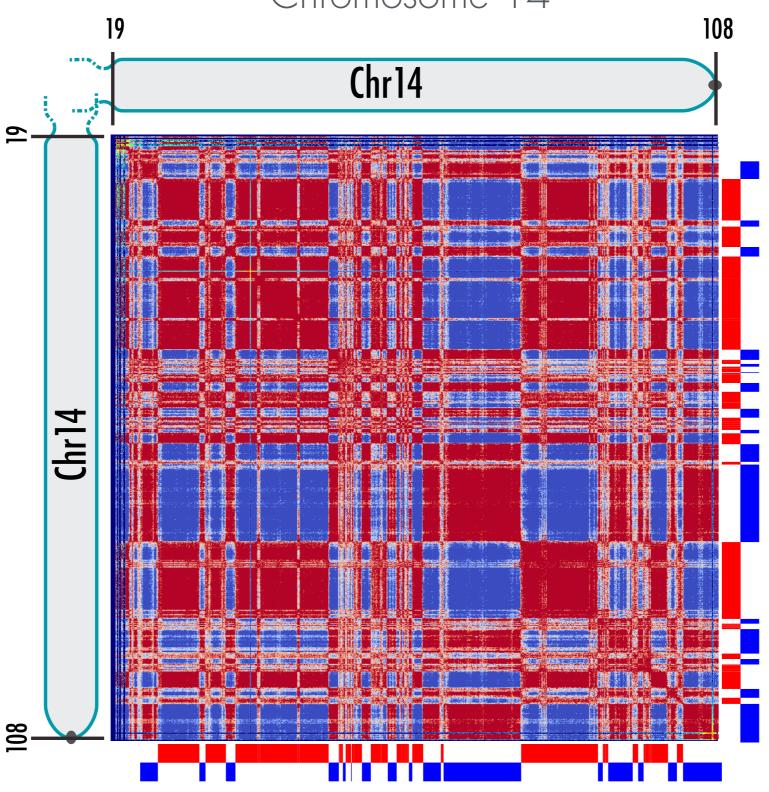






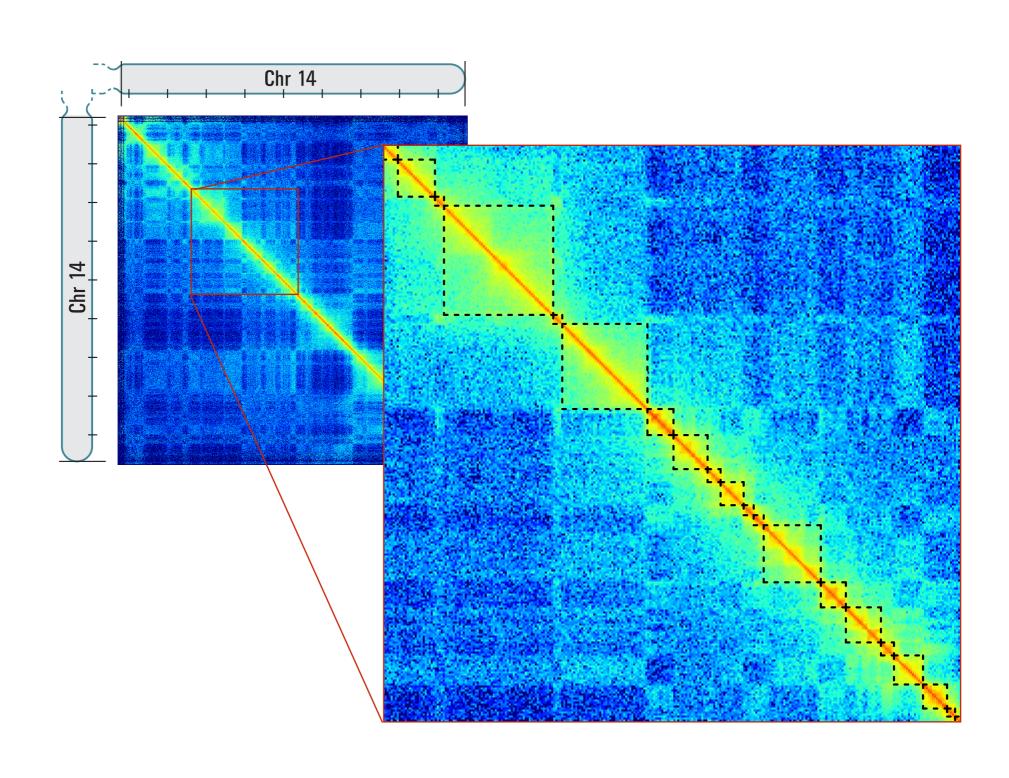


A/B Compartment Chromosome 14



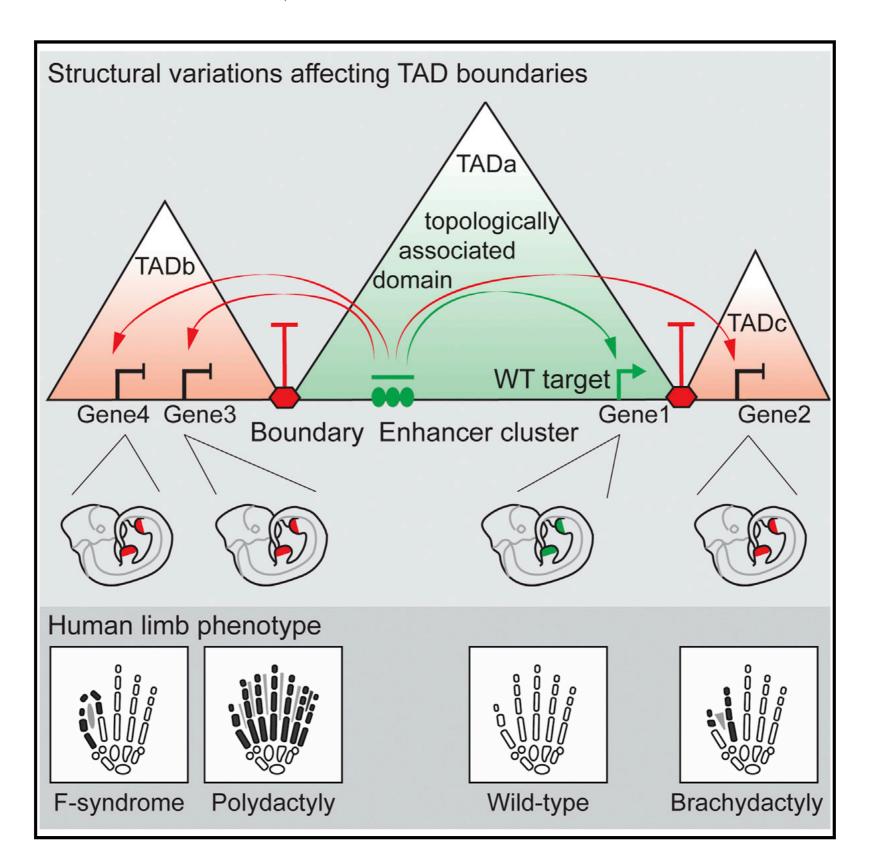
TADs

Chromosome 14



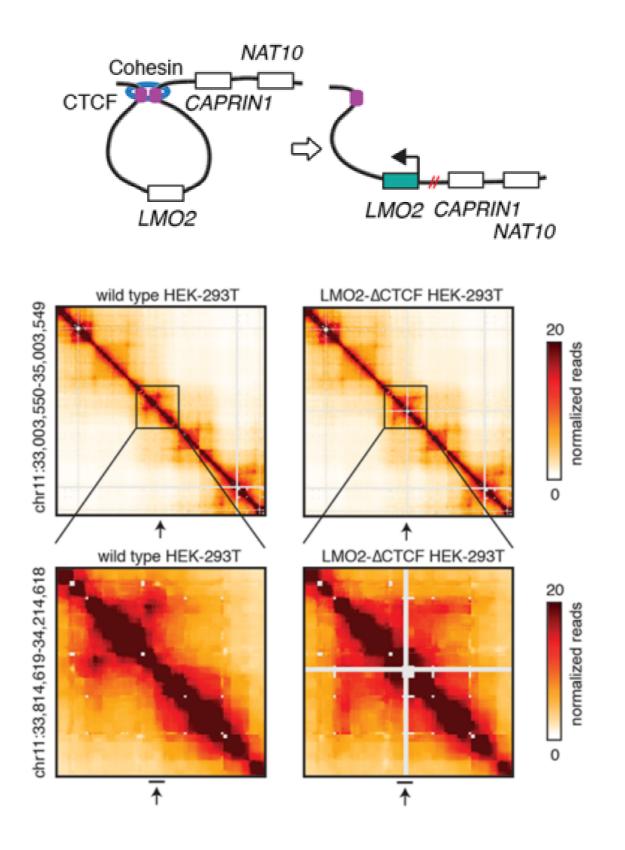
TADs are functional units

Lupiáñez, et al. (2015). Cell, 1-15.



TADs are functional units

Hnisz, D., et al. (2016). Science, on line



Many alternatives

Tool	Short-read aligner(s)	Mapping improvement	Read filtering	Read-pair filtering	Normalization	Visualization	Confidence estimation	Implementation language(s)	
HICUP [46]	Bowtie/Bowtie2	Pre-truncation	✓	✓	_	_	_	Perl, R	
Hiclib [47]	Bowtie2	Iterative	√a	✓	Matrix balancing	✓	_	Python	
HIC-inspector [131]	Bowtie	_	✓	✓	_	✓	_	Perl, R	
HIPPIE [132]	STAR	√b	✓	✓	_	_	_	Python, Perl, R	
HIC-Box [133]	Bowtie2	_	✓	✓	Matrix balancing	✓	_	Python	
HiCdat [122]	Subread	_c	✓	✓	Three options ^d	✓	_	C++, R	
HIC-Pro [134]	Bowtie2	Trimming	✓	✓	Matrix balancing	_	_	Python, R	
TADbit [120]	GEM	Iterative	✓	✓	Matrix balancing	✓	_	Python	
HOMER [62]	_	_	✓	✓	Two options ^e	✓	✓	Perl, R, Java	
Hicpipe [54]	_	_	_	_	Explicit-factor	_	_	Perl, R, C++	
HiBrowse [69]	_	_	_	_	_	✓	✓	Web-based	
Hi-Corrector [57]	_	_	_	_	Matrix balancing	_	_	ANSI C	
GOTHIC [135]	_	_	✓	✓	_	_	✓	R	
HITC [121]	_	_	_	_	Two options ^f	✓	✓	R	
chromoR [59]	_	_	_	_	Variance stabilization	_	_	R	
HiFive [136]	_	_	✓	✓	Three options ⁹	✓	_	Python	
Fit-Hi-C [20]	_	_	_	_	_	✓	✓	Python	

Many alternatives

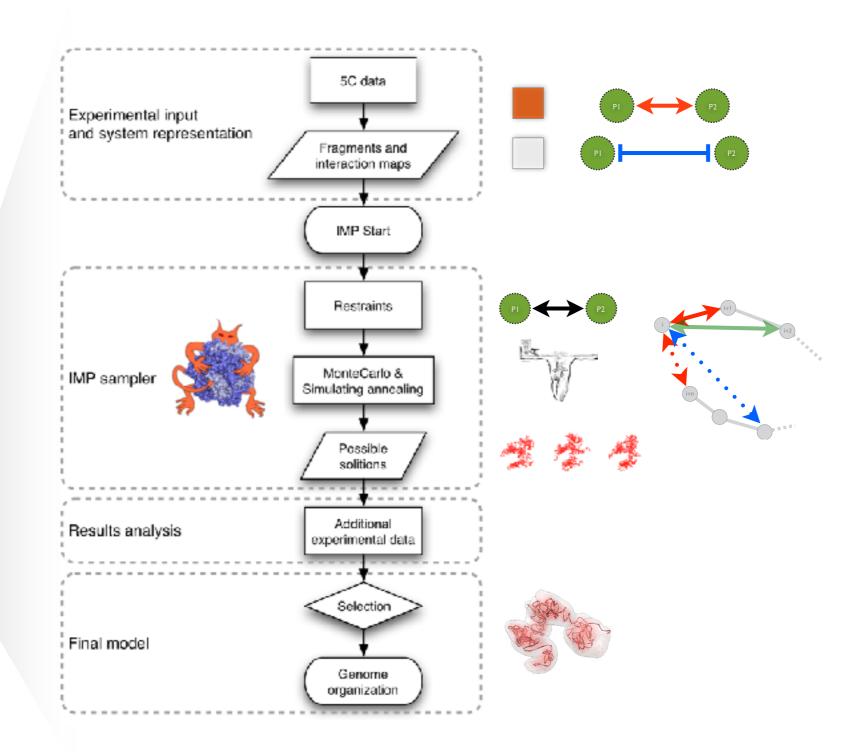
Method "available online	Representation	Scoring	Sampling	Models			
		U _{3C}			U _{Phys}		
		$F_{ij} \rightarrow D_{ij}$ conversion	Functional form				
ChromSDE* [37]	Points	$D_{ij} = \left\{ egin{array}{l} \left(rac{1}{F_{ij}} ight)^{lpha} & ext{if } F_{ij} > 0 \ \infty & ext{if } F_{ij} = 0 \end{array} ight. \ lpha & ext{is optimized} \end{array}$	$\sum_{\left(ij\right)D_{g}<\infty ight)} rac{\langle r_{ij}^{2}-D_{ij}^{2} angle}{D_{g}} -\lambda \sum_{\left(i,j\right)} r_{ij}^{2} \ ext{where} \ \lambda \ ext{is} $ set to 0.01		N/A	Deterministic semidefinite programming to find the coordinates	Consensu
ShRec3D* [38]	Points	$D_{ij} = \begin{cases} \left(\frac{1}{F_{ij}'}\right)^{\alpha} & \text{if } F_{ij}' > 0 \\ \frac{N^2}{\sum_{y,y}F_{iy}'} & \text{if } F_{ij}' = 0 \end{cases}$ $F_{ij}' \text{ is the original } F_{ij}' \text{ corrected to}$ $\text{satisfy all triangular inequalities with the shortest path reconstruction}$	N/A	N/A	N/A	Deterministic transformations of D _{ij} into coordinates	Consensu
TADbit* [43]	Spheres		$\sum_{(i,j)} k_{ij} (r_{ij} - D_{ij})^2$ where $k_{ij} = 5$ if	Yes	U _{excl} and U _{bond} have	Monte Carlo (MC)	Resamplir
		$D_{ij} \propto \begin{cases} \alpha F_{ij} + \beta & \text{if } F_{ij} < \gamma' \text{ or } F_{ij} > \gamma \\ \frac{S_i + S_j}{2} & \text{if } i - j = 1 \end{cases} $ α and β are estimated	$ i-j =1$ or proportional to F_{ij}		harmonic forms	sampling with Simulated annealing	
		from the max and the min F_{ij} , from the optimized max distance and from the resolution. $\gamma' < \gamma$ are optimized too. s_i is the radius of particle i	otherwise			and Metropolis scheme	
BACH* [45]	Points	$D_{ij} \propto rac{B_i B_j}{F_i^{\alpha}}$. The biases B_i and B_j and α are optimized	$b_{ij}D_{ij}^{1/2} + c_{ij} \log(D_{ij})$ where b_{ij} and c_{ij} are optimized parameters	No	No	Sequential importance and Gibbs sampling with hybrid MC and adaptive rejection	Populatio
Giorgetti et al. [40]	Spheres	Particles interact with pair-wise well potentials of depths B_{ij} a hard-core radius and smaller than a maximum contact radiu the population of models	No	N/A	MC sampling with metropolis scheme	Populatio	
Duan et al. [41]	Spheres	$\overline{F_{i-j}} = \frac{\sum_{k=j}^{N-j-j} F_{j(k+j-j)}}{N-(j-1)}$ is the average of F_{ij} at genomic distance	$\sum_{(i,j)} (r_{ij} - D_{ij})^2$	Yes	U _{excl} and U _{bond} have harmonic forms	Interior-point gradient- based method	Resampli
		$ i-j $ expressed in kb. $D_{ij} = \overline{F_{ i-j }} \times 7.7 \times i-j $ assuming that α 1 kb maps onto 7.7 nm			narmonic forms	based method	
MCMC5C* [49]	Points	$D_{ij} \propto \frac{1}{F_{ij}^x}$ where is optimized	$\sum_{(i,j)} (F_{ij} - r_{ij}^{-1/\alpha})^2$	N/A	N/A	MC sampling with Markov chain based algorithm	Resampli
PASTIS* [47]	Points	$D_{ij} \propto \frac{1}{F_{ij}^{\alpha}}$ where α is optimized	$b_{ij}D_{ij}^{1/2} + c_{ij}\log(D_{ij})$ where b_{ij} and c_{ij} are optimized parameters	No	No	Interior point and isotonic regression algorithms	Resampli
Meluzzi and Arya [48]	Spheres	$\sum_{(l,l)} k_{ij} r_{ij}^2$ where k_{ij} are adjusted such that the contact probabilities computed on the models match the F_{ij}			U _{excl} is a pure repulsive LJ potential. U _{bond} and U _{bend} have harmonic forms	Brownian dynamics	Resampli
AutoChrom3D* [44]	Points	$D_{ij} \propto \begin{cases} \alpha F_{ij} + \beta & \text{if } F_{\min} < F_{ij} < F_{\gamma} \\ \alpha' F_{ij} + \beta' & \text{if } F_{\gamma} < F_{ij} < F_{\max} \end{cases}$ where $F_{\min} (F_{\max})$ are the min(max) of F_{ij} . The parameters (α, β) , (α', β') and F_{γ} are found using the nuclear size, the resolution and the decay of F_{ij} with $ i-j $	$\sum_{\{i,j\}} \frac{\langle r_{ij} - D_{ij} \rangle^2}{D_{ij}^2}$	Yes	N/A	Non-linear constrained	Consensu
Kalhor et al. [14]	Spheres	$D_{ij} = R_{contact}$ to enforce the pair contact, if the normalized contact frequency F_{ij} is higher than 0.25. Otherwise the contact is not enforced	$\sum_{\text{models}} \sum_{(i,j)} k_{ij} (r_{ij} - D_{ij})^2$ where k_{ij} is different for pairs of particles, on different chromosomes, on the same chromosome, or connected	Yes	U _{excl} and U _{bond} have harmonic forms	Conjugate gradients sampling with Simulated annealing scheme	Populatio

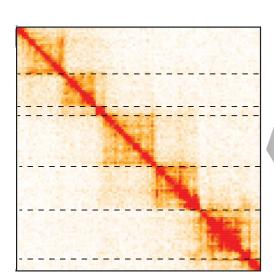
^{*} These methods are publicly available.



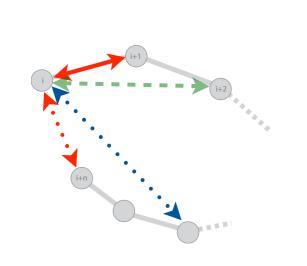


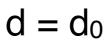
http://3DGenomes.org
http://www.integrativemodeling.org





Model representation and scoring

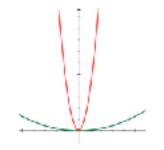






Harmonic

Harmonic
$$H_{i,j} = k \left(d_{i,j} - d_{i,j}^0 \right)^2$$

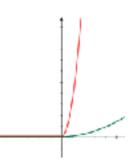


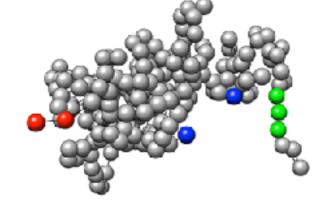




Harmonic Upper Bound

$$\begin{cases} if \ d_{i,j} \ge d_{i,j}^0; & ubH_{i,j} = k \left(d_{i,j} - d_{i,j}^0 \right)^2 \\ if \ d_{i,j} < d_{i,j}^0; & ubH_{i,j} = 0 \end{cases}$$

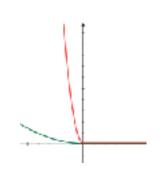




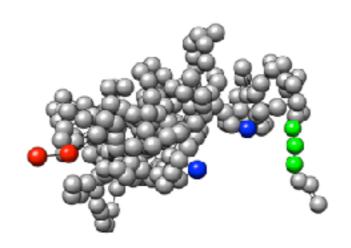


Harmonic Lower Bound

$$\begin{cases}
if \ d_{i,j} \le d_{i,j}^{0}; & lbH_{i,j} = k(d_{i,j} - d_{i,j}^{0})^{2} \\
if \ d_{i,j} > d_{i,j}^{0}; & lbH_{i,j} = 0
\end{cases}$$

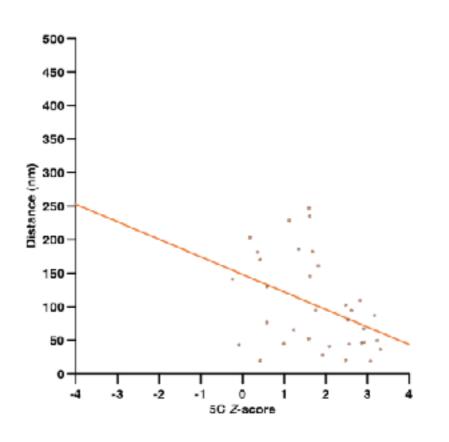


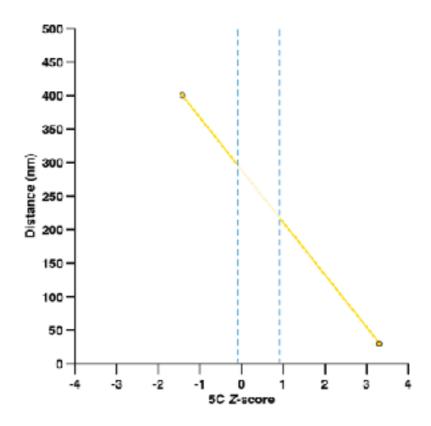
From 3C data to spatial distances



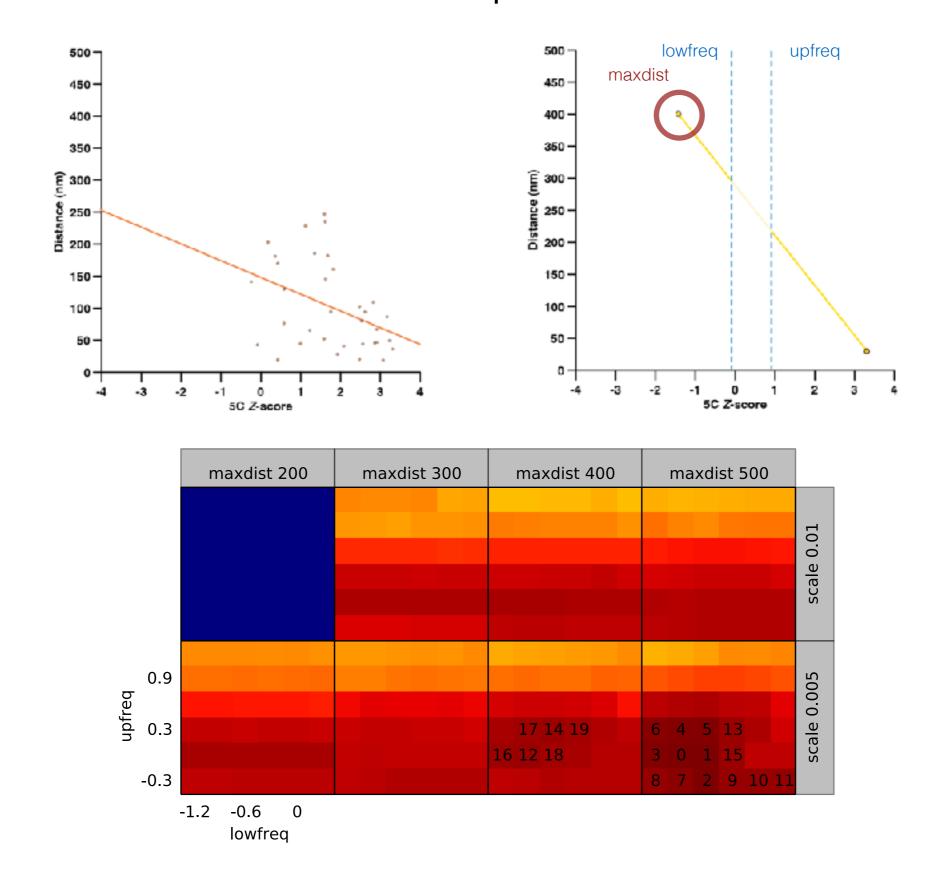
Neighbor fragments

Non-Neighbor fragments

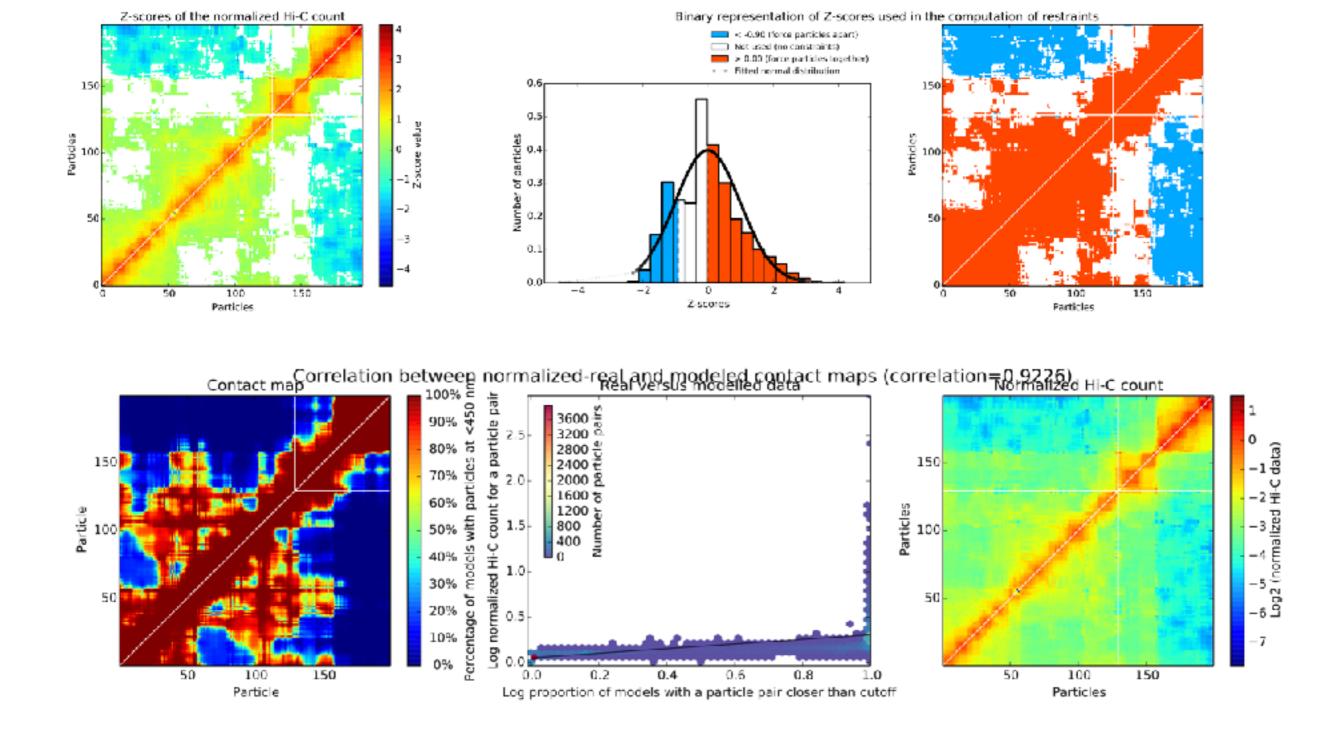




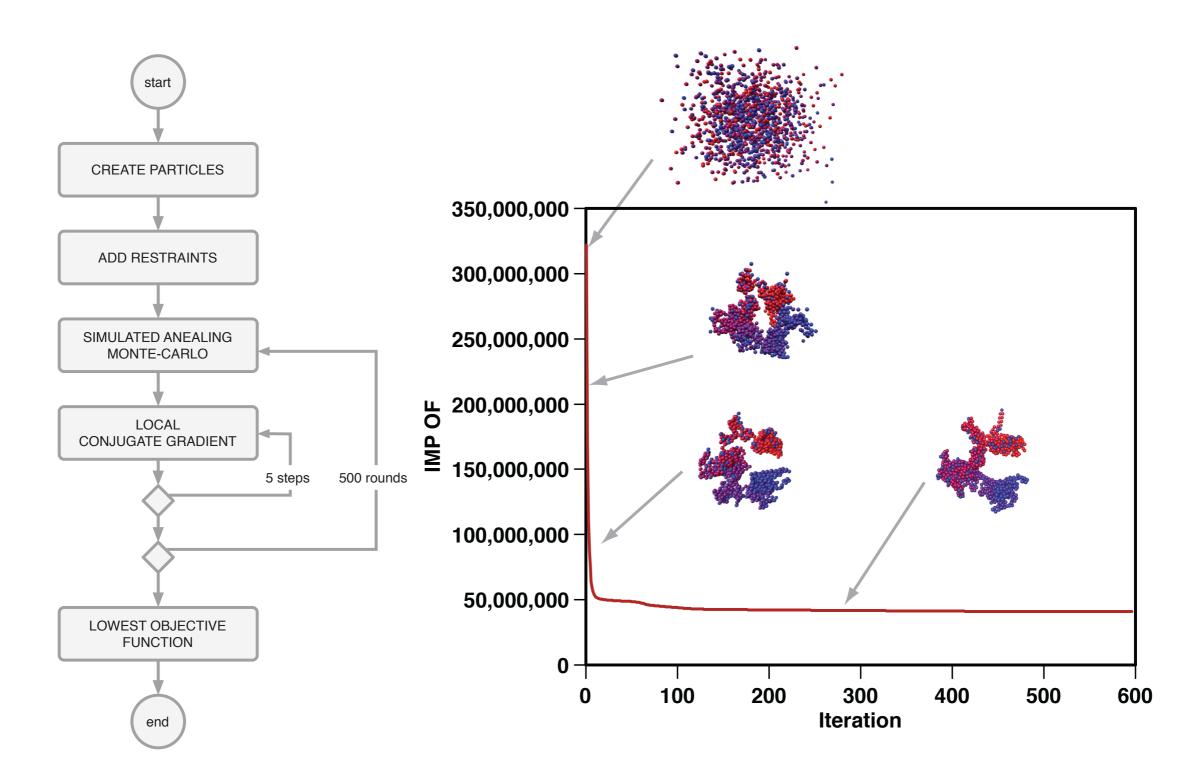
Parameter optimization



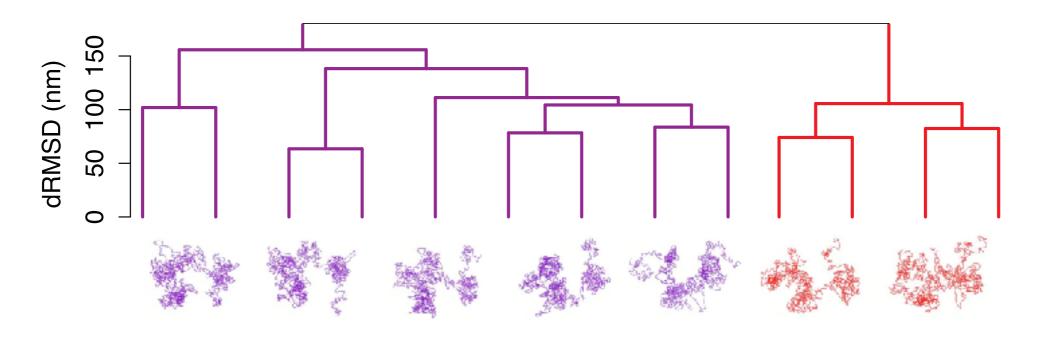
Parameter optimization



Optimization of the scoring function



Model analysis: clustering and structural features

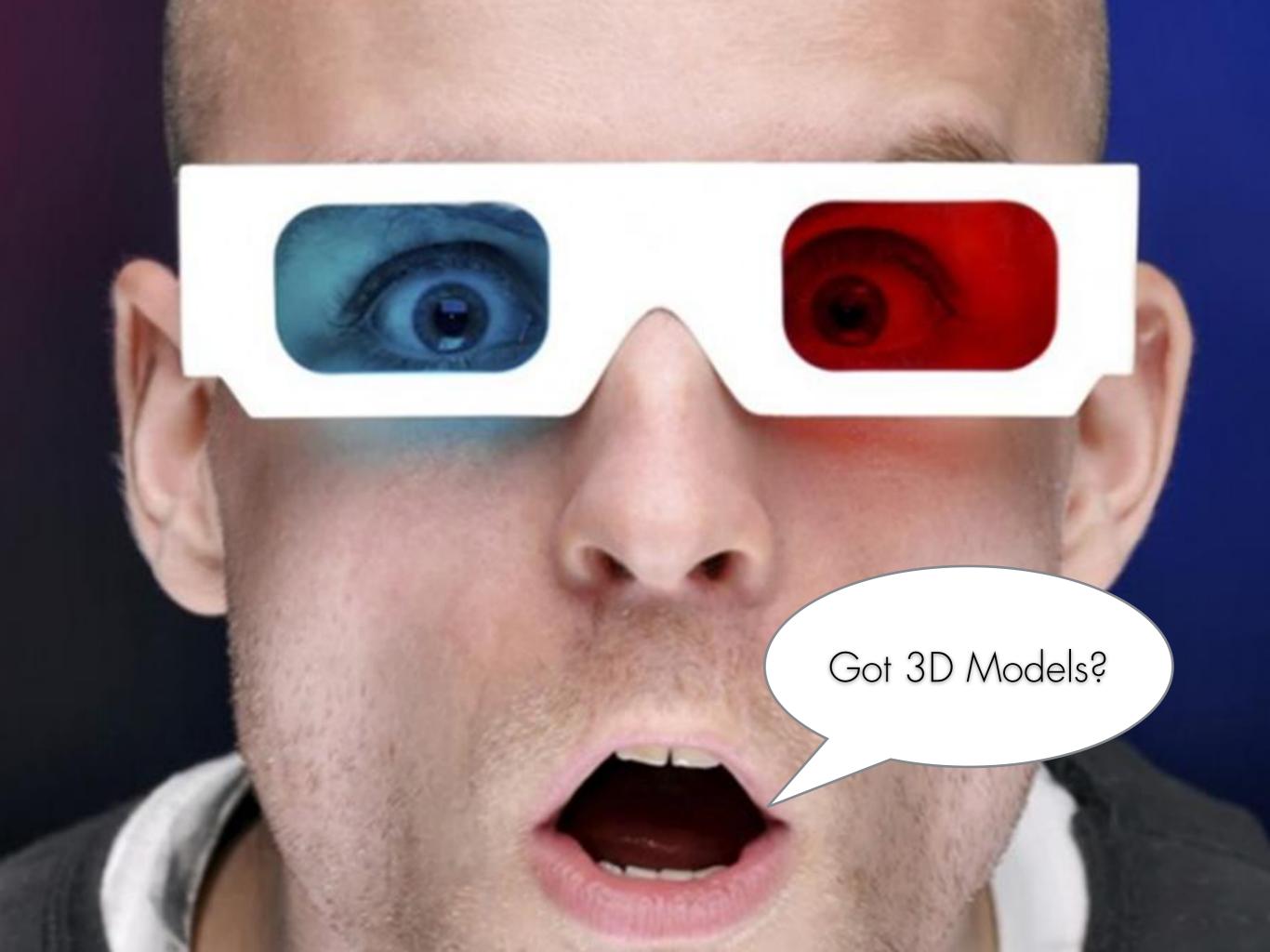


Accessibility (%)

Density (bp/nm)

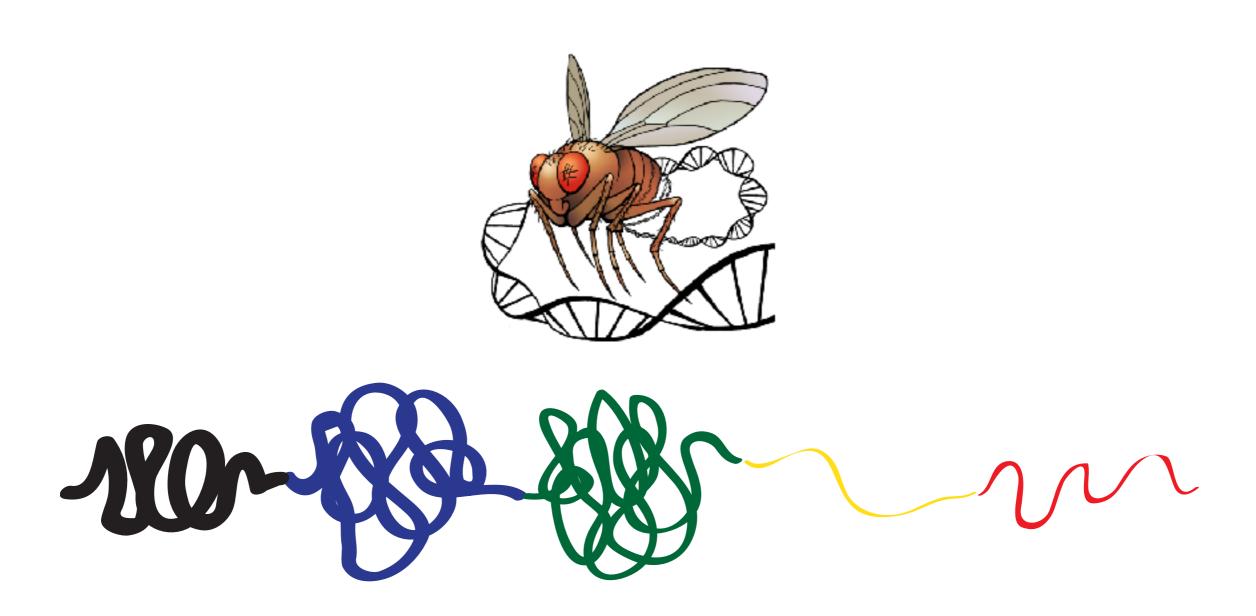
Interactions

Angle



Structuring the COLORs of chromatin

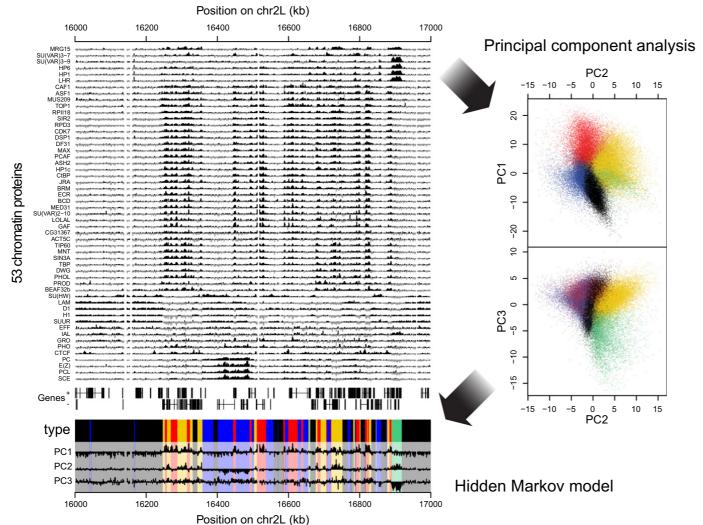
Serra, Baù et al. (2017) PLOS CompBio.

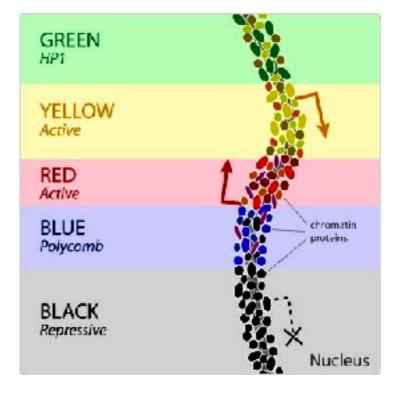


Fly Chromatin COLORs

Filion et al. (2010). Cell, 143(2), 212-224.

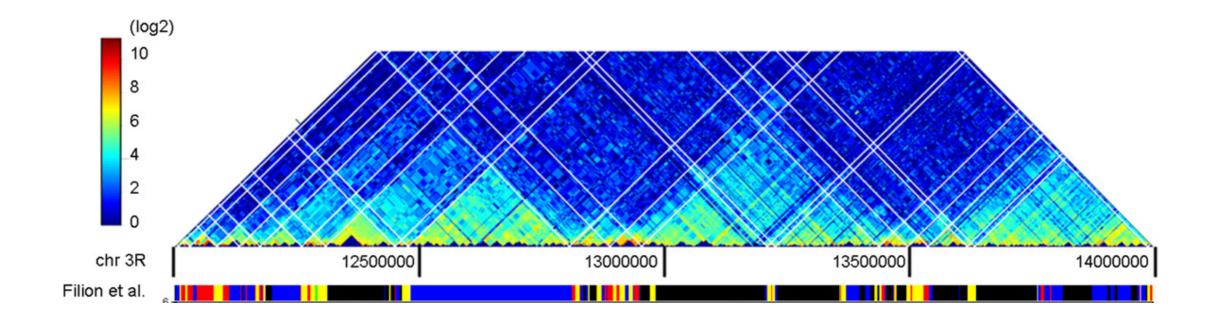


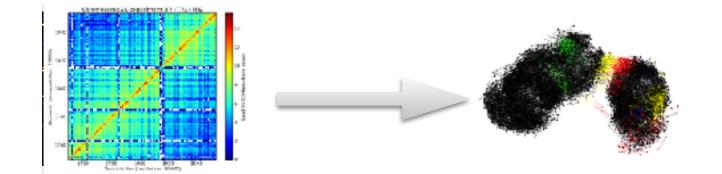




Fly Chromatin COLORs

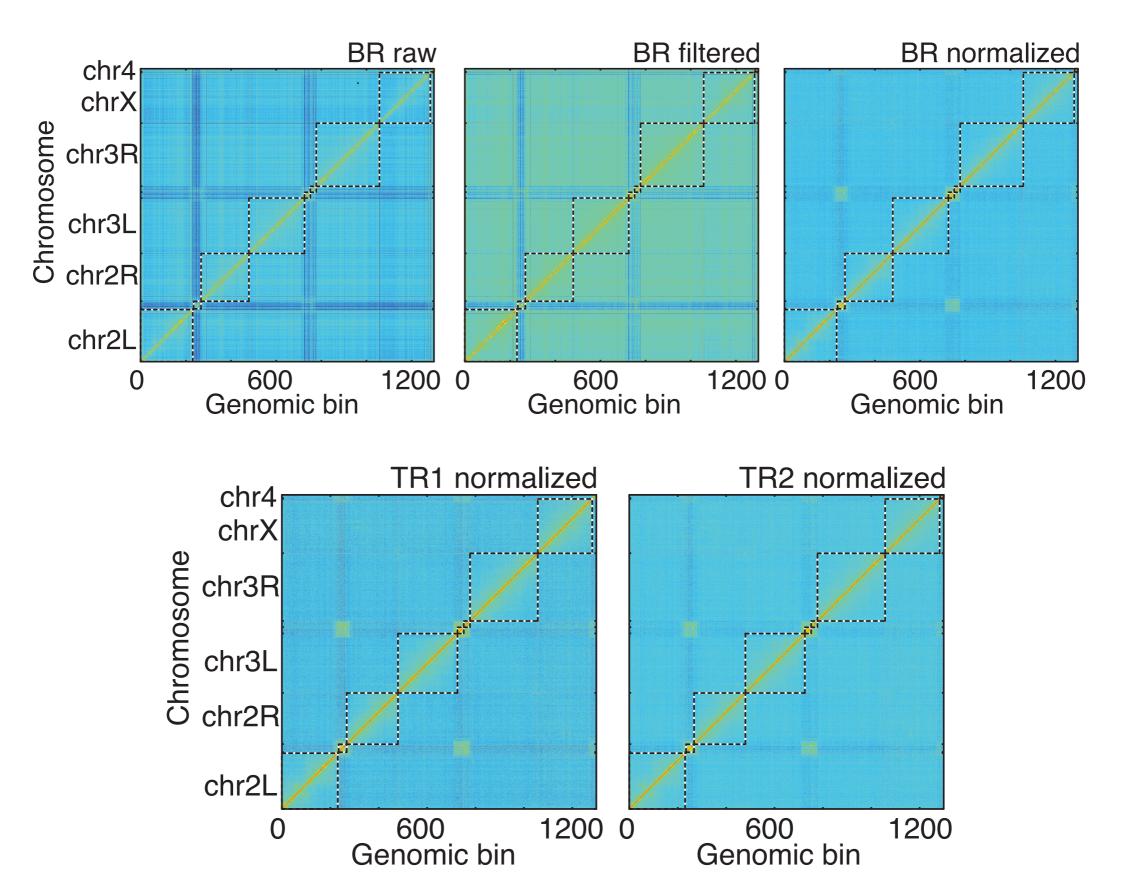
Hou et al. (2012). Molecular Cell, 48(3), 471–484.



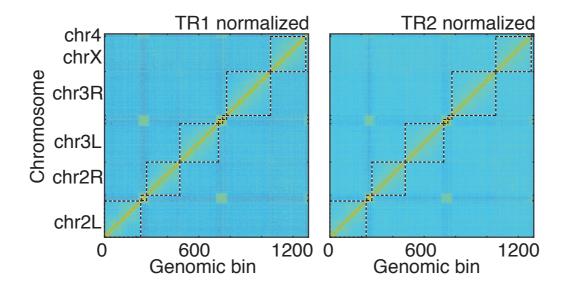


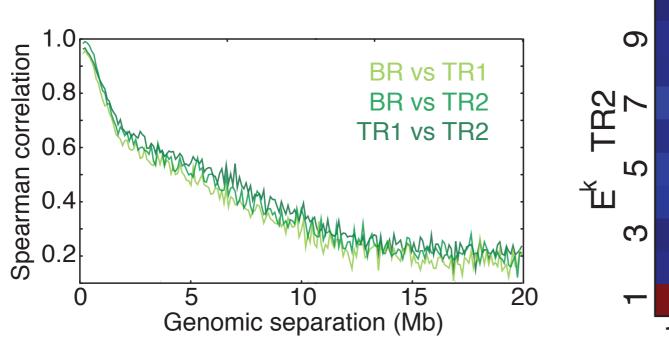
~200 regions of ~5Mb each 2Kb resolution

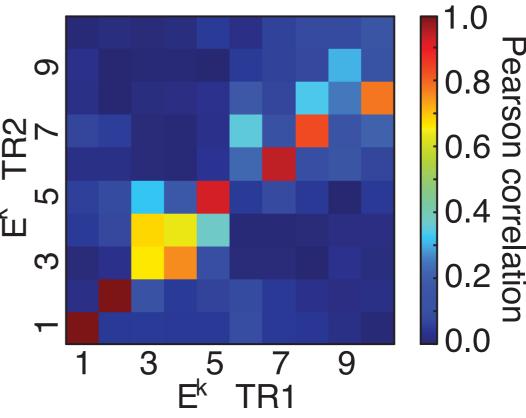
Mapping · Filtering · Normalizing



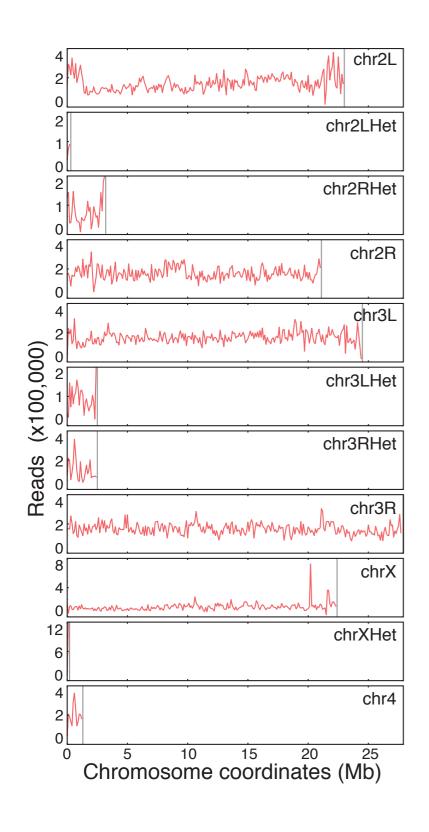
Matrix comparison

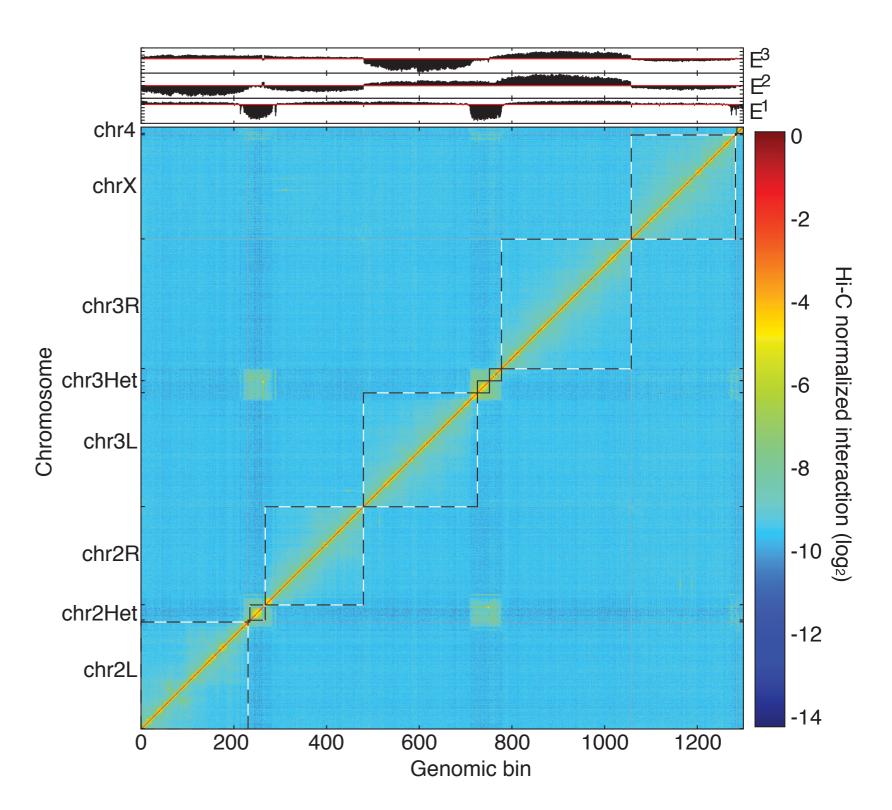




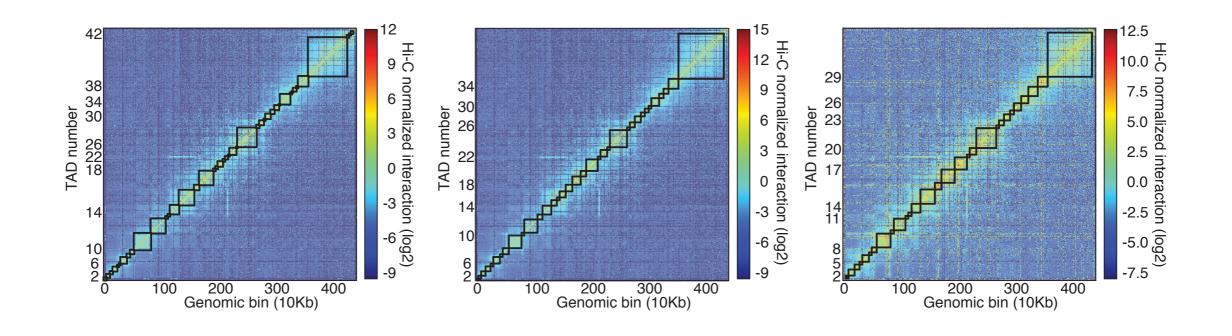


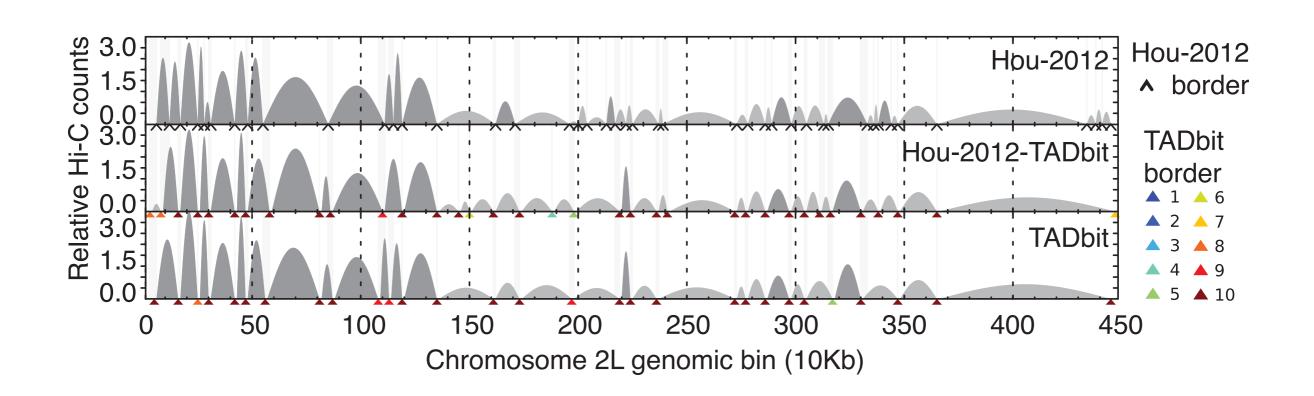
Matrix merging





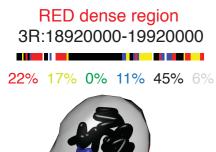
TAD detection · comparison

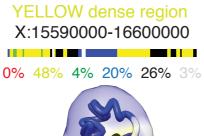




Structural properties

50 1Mb regions. 10 enriched for each color.



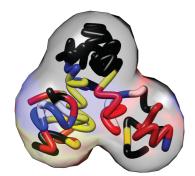


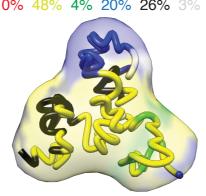


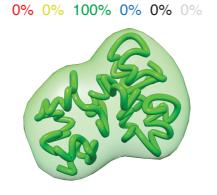


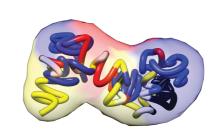
BLACK dense region 2L:17500000-18530000

1% 0% 0% 0% 98% 1%



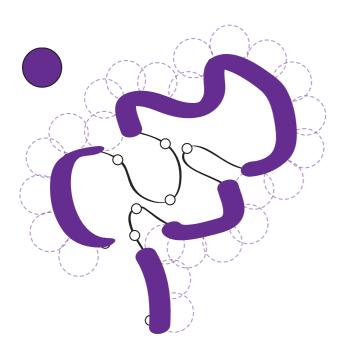




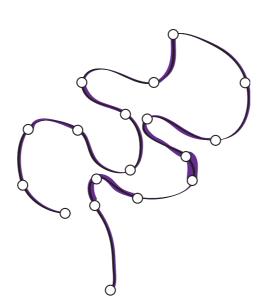




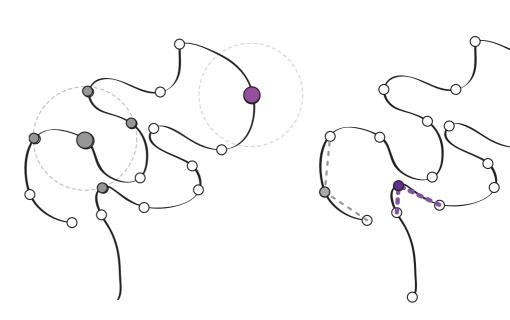
Accessibility (%)



Density (bp/nm)

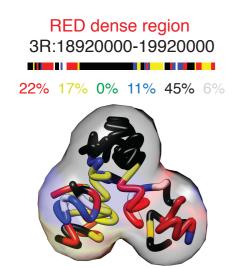


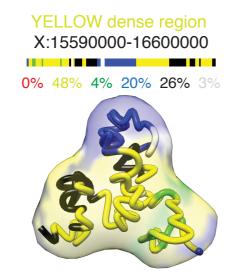
Interactions

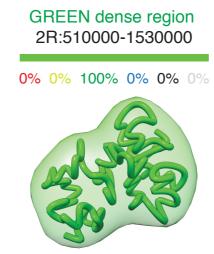


Angle

Structural COLORs

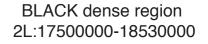






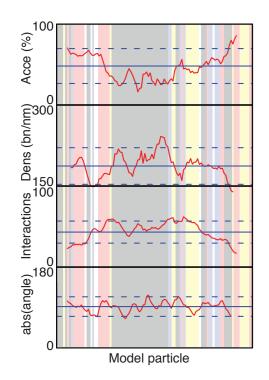


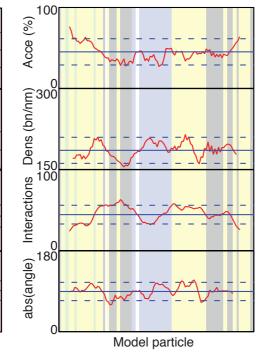


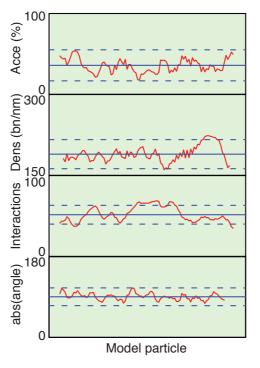


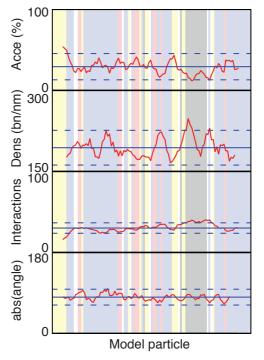
1% 0% 0% 0% 98% 1%

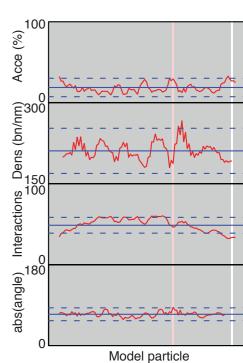




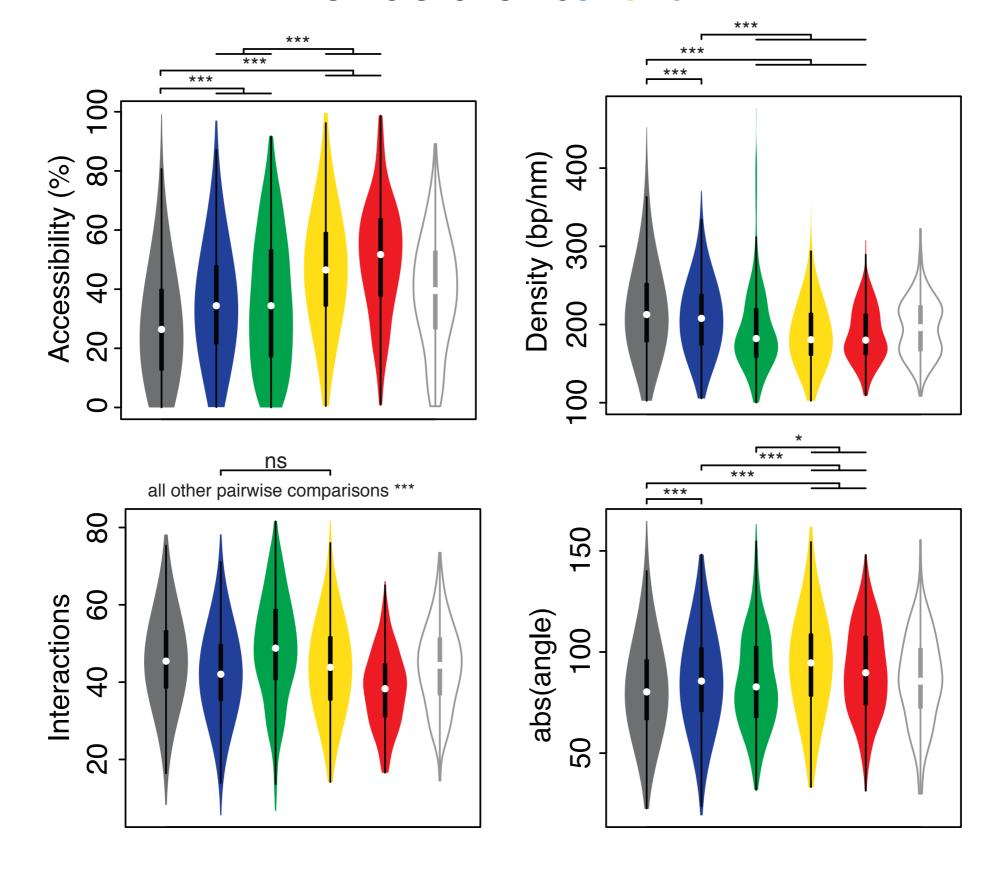




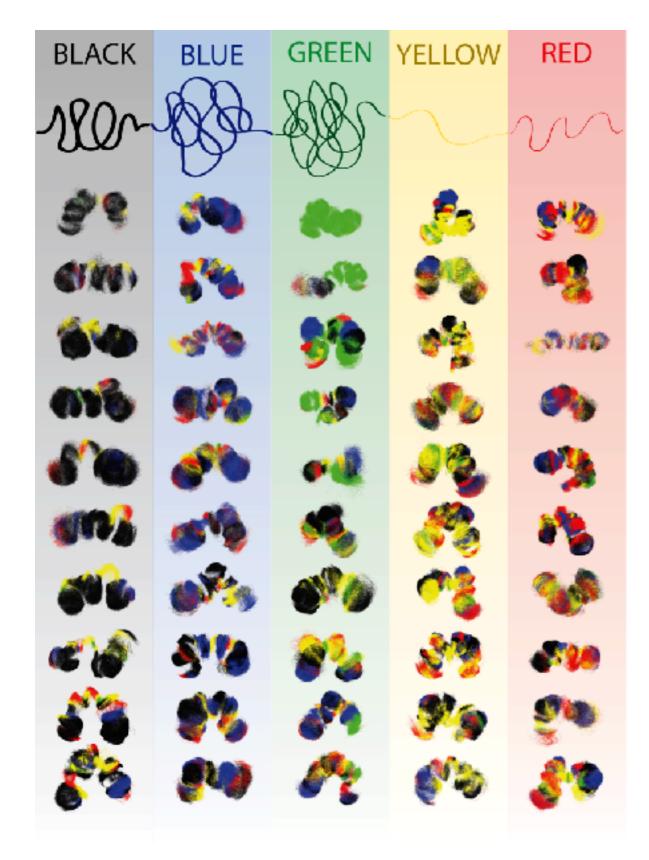


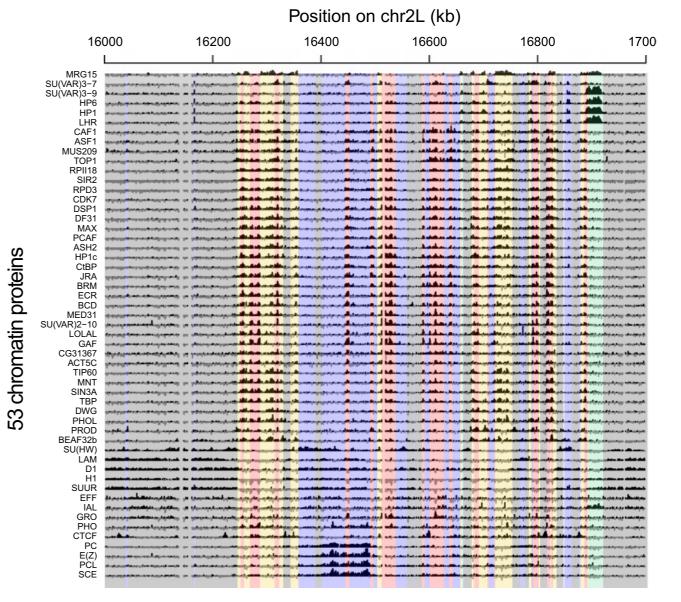


Structural COLORs



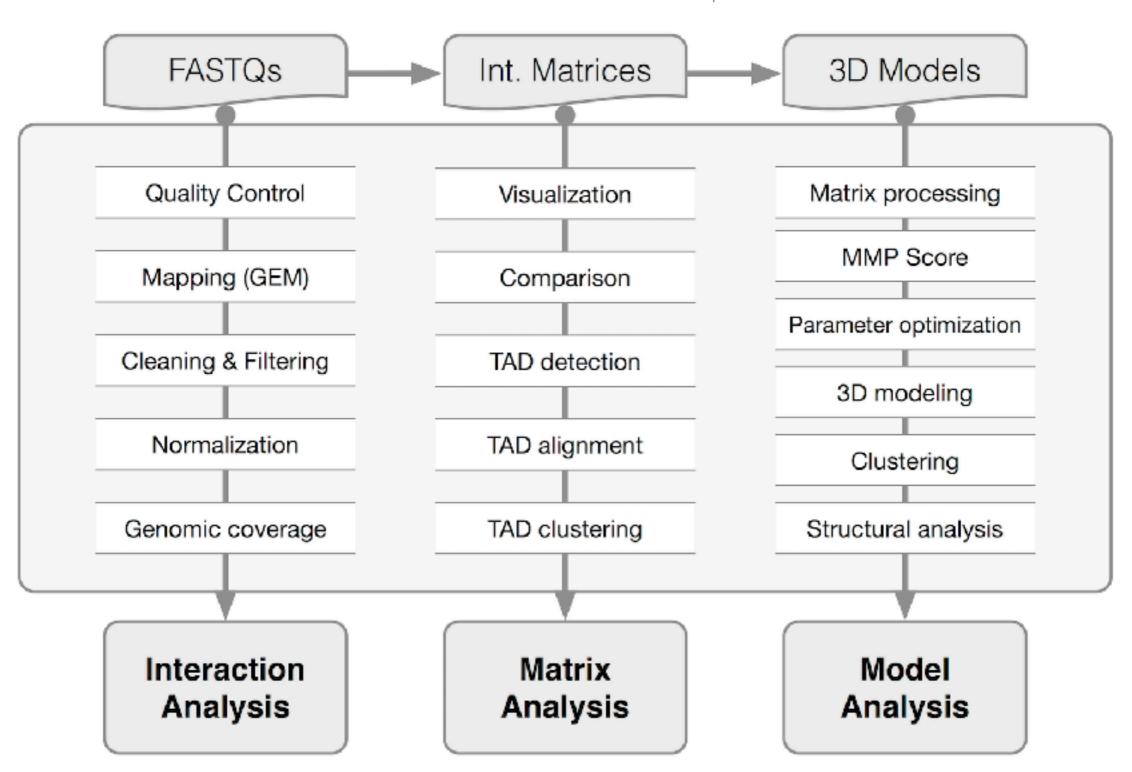
Structural COLORs







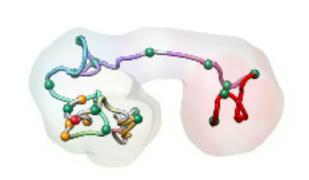
Serra, Baù, et al. (2017). PLOS CompBio

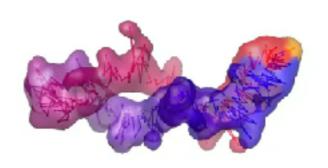




Baù, D. et al. Nat Struct Mol Biol (2011)
Umbarger, M. A. et al. Mol Cell (2011)
Le Dily, F. et al. Genes & Dev (2014)
Trussart et al. Nature Comm. (2017)
Cattoni et al. Nature Communication (2017)



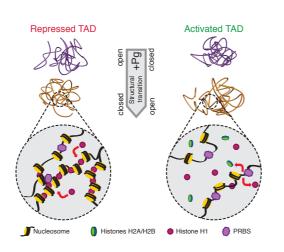


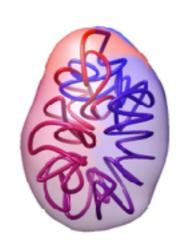




Distinct structural transitions of chromatin topological domains correlated with coordinated hormone-induced gene regulation.

Framework trade of the control of the contro









David Castillo
Yasmina Cuartero
Irene Farabella
Silvia Galan
Mike Goodstadt
Julen Mendieta
Francesca Mugianesi
Juan Rodríguez
François Serra
Paula Soler
Aleksandra Sparavier
Yannick Spill
Marco di Stefano

Former members: Davide Baù & Marie Trussart

http://sgt.cnag.cat/www/presentations/















